

Forecasting Research

Forecasting Research Division
Scientific Paper No. 33

The Meteorological Office mesoscale data assimilation scheme

by

B. Macpherson, B.J. Wright, W.H. Hand and A.J. Maycock

May 1995

**Meteorological Office
London Road
Bracknell
Berkshire
RG12 2SZ
United Kingdom**

ORGS UKMO F

National Meteorological Library
FitzRoy Road, Exeter, Devon. EX1 3PB

**Forecasting Research Division
Scientific Paper No. 33**

**The Meteorological Office
mesoscale data assimilation scheme**

by

B. Macpherson, B.J. Wright, W.H. Hand and A.J. Maycock

May 1995

The Meteorological Office mesoscale data assimilation scheme

By B. Macpherson, B.J. Wright, W.H. Hand & A.J. Maycock

Forecasting Research Division, Meteorological Office, Bracknell

SUMMARY

Although based on the same fundamental approach to data assimilation as the global and regional model schemes, the mesoscale version of the Meteorological Office data assimilation system receives a more varied observational input than its larger scale counterparts. Several surface data types are assimilated only at mesoscale resolution. Also, a moisture observation pre-processing system blends information from satellite imagery, radar and surface cloud reports with a model forecast to produce humidity soundings for assimilation by the model. Particular problems connected with cloud top height assignment from infrared imagery are explained, along with solutions devised to overcome them. Examples are given of the impact on analyses and forecasts from assimilating these various mesoscale data sources.

1. INTRODUCTION

Within its suite of operational numerical weather prediction (NWP) models, the UK Meteorological Office (UKMO) runs a mesoscale model with the aim of adding local detail to forecast guidance on weather in the UK up to one day ahead. The global and regional models, with grid-lengths of around 100km and 50km respectively, cannot resolve the topographic variations across the UK which may influence the local weather within some larger scale system. With a grid-length of 17km, the mesoscale model is designed to supply this finer scale information, at least in slowly moving situations when the model's evolution is less constrained by the boundary conditions which come from the regional model.

With the emphasis being on prediction of weather elements rather than the large scale flow pattern, conditions near the surface and the moisture distribution are of prime importance. These two aspects have received greatest attention in the development of the data assimilation system for the mesoscale model. It employs the same "Analysis Correction" (AC) data assimilation scheme (Lorenc *et al.* 1991) as the regional and global configurations, but with some extra data not available to the larger scale models. Surface observations of temperature, humidity and wind over land are at present assimilated only in the mesoscale version. High resolution model orography is desirable to resolve features represented by these surface data.

While surface observations are reasonably plentiful, the conventional observing network has poor spatial coverage for the purpose of moisture analysis. The global and regional models receive their humidity information from radiosondes, which are at least 300km apart.

Satellite imagery can provide data at much better horizontal resolution, but its direct use in operational models is not yet common. In the tropics, where convective rainfall dominates, promising impacts have been obtained with proxy rainfall observations derived from OLR (Outgoing Longwave Radiation) measured by geostationary satellites (Puri and Miller 1990, Krishnamurti *et al.* 1991, Krishnamurti *et al.* 1994). In such schemes, the moisture analysis is adjusted so that the convective parametrisation will yield the 'observed' precipitation rate. Another way to exploit satellite imagery has been adopted successfully in mid-latitudes and applies also to non-precipitating cloud. In this technique, a cloud classification is carried out on the imagery and 'synthetic' humidity profiles are assigned to the different features in the image, based on earlier statistical analyses of imagery and collocated radiosondes. An example in this category was the study of Mills and Davidson (1987), who demonstrated forecast improvements over Australia with infrared data. Garand (1993) also analysed visible and water vapour channels in the 'Humsat' retrieval algorithm, which generates humidity data on six standard pressure levels from 1000-300mb. These data have significantly improved the moisture analysis over the oceans in the Canadian regional model (Chouinard *et al.* 1994).

An approach to moisture initialisation closer to that described in this paper has been applied to mesoscale simulations of convective cloud systems over Florida (Zack *et al.* 1988, Young and Zack 1994). In this case, infrared imagery is used to derive cloud cover and cloud top height, surface reports to estimate cloud base and radar to decide where the model profiles should be moist enough to produce precipitation. The range of moisture data embraced by this system corresponds closely with that described in Section 4 of this paper, although there are differences in the way the various data types are treated.

At the UKMO, it is currently only the mesoscale model that makes routine objective use of satellite imagery for cloud analysis, although an imagery product for the regional model assimilation system has recently been tested (Richards and Bell 1994). The mesoscale assimilation system is shown schematically in Figure 1. Conventional data, including the additional surface data described in Section 3, are assimilated directly into the model. Meteosat infrared imagery, radar rainfall imagery and surface cloud reports are combined with the latest 3-hour model forecast in MOPS, the Moisture Observation Pre-processing System (Wright 1993). The main output from MOPS consists of a 3-dimensional analysis of cloud fraction. This is converted into a set of relative humidity soundings at each model grid-point, which are then assimilated in much the same way as radiosondes.

The data assimilation process is continuous, with eight 3-hourly assimilation cycles in each 24-hour period. Each cycle produces an analysis which becomes the start field for the next cycle. The forecast model is run four times daily, from data times of 0, 6, 12, and 18 UTC. The 0 and 18 UTC forecasts finish at $t+18$, the 12 UTC forecast runs to $t+24$ and the 6 UTC run extends to $t+30$. Boundary conditions are taken from the regional model forecast with the same data time.

In the following sections we describe the distinctive features of the mesoscale system in more detail, along with examples of the impact on analyses and forecasts from the separate components.

2. FORECAST MODEL

The UKMO mesoscale model is a version of the unified forecast/climate model (Cullen 1991) with a grid spacing of 0.15 degrees ($\approx 17\text{km}$) and 31 levels. Figures 2 and 3 compare its horizontal and vertical resolution with those of the regional configuration (Although Figure 3 shows heights in metres, the model has a hybrid vertical co-ordinate, giving sigma levels in the lower troposphere and pressure levels in the stratosphere). At mesoscale resolution, the representation of orography and the coastline are quite realistic (Figure 4), although individual peaks and valleys less than 35km across cannot be represented.

When implemented operationally in December 1992, the physical parametrisations in the mesoscale configuration were different in a number of respects from their counterparts in the regional and global models. A revised boundary layer scheme and new treatment of convective downdraughts had been developed first for the low resolution 'climate' model. These parametrisation improvements, along with an enhanced (orographic) surface roughness specification, were required by the new mesoscale model in order for it to match the performance of its predecessor. The development and operational trials of the model are described by Ballard *et al.* (1993). Over the last two years, in keeping with the philosophy of a 'unified' model, the parametrisations of the mesoscale, regional and global models have been brought closely into line with each other. The main exception is that gravity wave drag effects are not included in the mesoscale model.

Although data assimilation developments have focused on new data, it should be noted that the higher resolution of the mesoscale model does give some benefits within the data assimilation system. The main example of this is a consequence of improved vertical resolution, which allows higher resolution radiosonde profiles to be assimilated, leading to better vertical temperature and moisture structure (Figure 5). The benefit cannot be achieved by simply running a high resolution model from an interpolated large-scale analysis; the higher resolution of both the data and the assimilating model are essential.

Significant differences between the surface pressure analyses of the mesoscale and regional models are very rare, but, on occasion, the mesoscale model's higher resolution can help capture the intensity of a small-scale system more accurately (Figure 6). In the case shown there, the impact from higher model resolution (Figure 6(d)) is larger than the impact from extra surface data present in the mesoscale run.

3. SURFACE DATA

(a) Temperature observations

Over land, screen temperature data are assimilated in the mesoscale model. The model background value is derived at a height of 1.5m above the surface. Before comparison with the model value, the raw observation is corrected by a standard lapse rate for differences between station height and the height of model orography. This correction is found to reduce the overall rms (observation-background) difference by around 0.2K. The observation increment at 1.5m is added to the surface temperature field T_s and, with decreasing weight in the vertical, to the lowest 6 levels of the model temperature field. The vertical correlation

function has a value of about 0.4 at level six near 950mb. Standard techniques for statistical analysis of (observation-background) differences (Daley 1991) led to a horizontal forecast error correlation scale of approximately 100km, this being the parameter s in the equation for the correlation function μ used by the AC scheme:

$$\mu = (1 + r/s) \exp(-r/s) \quad (1)$$

where r is distance. The observation error, dominated by representativeness, was deduced to be 1.1K. The rms fit to the data achieved in the analysis is close to this figure during the day, but a slightly poorer fit at night time takes the overall figure to 1.3K.

Benefit from assimilation of screen temperature data is greatest in anticyclonic situations. Figure 7 shows some impact results in a group of cases in which anticyclonic conditions dominate. A significant reduction in error of 13% at $t+9$ comes through assimilating the data, and a small signal is still present at $t+18$. The cases chosen contained extremes of winter cold, which explains the rather larger analysis errors than those quoted above. Also, the unexpected *decrease* in error between $t+0$ and $t+6$ deserves comment. This is because some of the winter cases had analysis times of 6 UTC, corresponding to the time of minimum temperature (and maximum model error), whereas model temperature errors in winter are smaller around midday ($t+6$).

(b) Humidity observations

Screen level dew point data are presented to the assimilation as relative humidity observations, and these have proved useful for defining areas of poor visibility, the analysis and prediction of which is one of the main goals of the mesoscale model. A good example is in Figure 8, where the surface data improve the forecast for southern England. The model diagnostic used for fog prediction is a 'fog fraction', which can be interpreted as the probability of visibility of less than 1km within the model grid-square (Clark *et al.* 1994). A model fog fraction of greater than 20% has been found to correspond well with observed areas of radiation fog. The vertical spreading of surface humidity increments is identical to that for temperature data, but the horizontal scale is slightly smaller at 75km.

(c) Wind observations

Surface wind data from ships are assimilated in all configurations of the unified model, but synop wind reports over land are used only by the mesoscale version. The latter are assumed to give values at a height of 10m and increments are spread upwards with decaying weight to around 400m. A 'blacklist' is maintained of stations in coastal and mountainous regions, where the local orography, and hence wind direction, are not representative of a 17km grid-box. Despite the elimination of unrepresentative stations, the 10m wind data have very little impact on the forecast wind field in general (Maycock 1993). In the unusual case shown in Figure 6, some benefit from synop wind data was noted in surface pressure. The 1.9mb impact at $t+6$ (Figure 6(e)) appears to come from data near the centre of the depression over southern Ireland at analysis time six hours earlier. The result is a slightly deeper depression, as required.

A possible explanation for the general lack of impact from the data emerges from a study of

the horizontal correlations of model background errors in 10m wind. Assuming that wind error correlations are isotropic, the simplest way to represent them is in terms of wind components along and perpendicular to the direction from observation point to grid point. With the assumption that equation (1) holds for streamfunction errors, this leads (Bell *et al.* 1993) to correlations between two longitudinal (LL) or transverse (TT) error components as follows:

$$\mu_{LL} = \exp(-r/s) \quad (2a)$$

$$\mu_{TT} = \mu_{LL} \{1 - \gamma(r/s)\} \quad (2b)$$

where γ is a parameter between zero and unity which measures the degree of non-divergence. If $\gamma=1$, the correlations are completely non-divergent and μ_{TT} goes negative beyond $r=s$. If $\gamma=0$, they are completely irrotational and $\mu_{TT} = \mu_{LL}$. Results of a statistical analysis of mesoscale model errors (Figure 9) show $\gamma=0$ as the 'best-fit'. The implication is that the model is insensitive to the data because it has difficulty in retaining information on the *divergent* wind from observations, tending to generate its own divergent wind structure instead.

(d) Hourly observations

All the above surface data types, along with surface pressure, are assimilated hourly into the mesoscale model, whereas the regional model assimilates surface pressure data every three hours. Some surface stations only report every three hours, so the data volume with hourly data is only about twice that for assimilation of 3-hourly data. The absence of reports at intermediate hours in some areas means that the normal 3-hour time window for nudging of data cannot be reduced to one hour without degrading the analysis. A compromise value of 2 hours is found to be satisfactory. One would look for some benefit from higher data frequency in fast moving situations, although these are unfortunately the cases where surface data have least overall impact. Increased data frequency for the upper-air would be more likely to give improvements in the forecast. In the case in Figure 6, the increase from 3-hourly to hourly surface pressure and synop wind data generates only a 1.3mb difference at $t+6$ (Figure 6(f)).

4. MOISTURE OBSERVATION PRE-PROCESSING SYSTEM (MOPS)

(a) Overall strategy

MOPS has been designed as a pre-processing system for several observation types with very different spatial coverage, error characteristics and relationships to model moisture variables. Since the MOPS cloud analysis includes model background information, the assimilation of MOPS data may properly be termed 'analysis nudging', as distinct from 'observation nudging'. With 'analysis nudging', there is a danger in data sparse regions of reinforcing a model forecast which may be in error. There are several reasons why this conceptually less satisfactory approach has been adopted in preference to individual inclusion of each data type for 'observation nudging' in the Analysis Correction scheme alongside more conventional data.

The first, at least in a chronological sense, relates to the origin of MOPS in the Interactive Mesoscale Initialization (IMI) system (Wright & Golding 1990) for an earlier version of the mesoscale model (Golding 1990). The IMI provided initial conditions for the previous model, which were a weighted combination of model first-guess fields and observations. When the new model was developed during 1992, it gave a shorter development path to adopt the core of this existing IMI system but with a new interface to the model via the assimilation technique described in Section 5. A moisture nudging study with the old mesoscale model by Segami (1992) had also given some encouragement that such a strategy would be fruitful.

Since the new model has been operational, the 'analysis nudging' strategy has been reviewed. There are a couple of factors influencing its retention at present. A nowcasting system called Nimrod is under development at UKMO to give 0-6 hour forecast guidance for the UK and surrounding waters. Very short period predictions will be generated by extrapolation from analyses and merged with model forecasts to produce the best overall forecast product. For cloud forecasts, the cloud fraction analysis from MOPS is a convenient starting point and the model background contribution is necessary to supply information in areas and at levels of the atmosphere where data are lacking. Another project underway at UKMO is to build a completely new data assimilation system based on variational analysis (Lorenc 1986 and Lorenc 1994). With such a major change in prospect, it has been judged best to leave more 'direct' assimilation techniques for the diverse 'raw' data sources in MOPS until they can be developed in a variational analysis context.

(b) Precipitation rate

As indicated in Figure 1, the sequence within MOPS begins with an analysis of precipitation rate. The primary input is a quality controlled radar rainfall image, prepared at a resolution of 5km and then averaged onto the model grid. The image is a composite from the 15 weather radars currently making up the UK network. Also used are present weather reports and hourly accumulations. A 3-hour mesoscale model forecast provides the background field, but is given no weight within the radar area. The analysis is performed by a 2-dimensional recursive filter technique (Hayden and Purser 1988), which imposes Gaussian smoothing with an effective scale of 35km within the radar area. Rates below 0.02mmhr^{-1} are set to zero at the end of the analysis.

As described in (c) below, the rainrate analysis is used to make inferences about total cloud cover. To help in this, a fractional precipitation cover is extracted for each model grid-point within the radar domain by assuming that all 5km pixels with values greater than 0.1mmhr^{-1} have full cover. The rainrate analysis is also applied to make adjustments to the multi-level cloud analysis, as explained in (f) below.

(c) Total cloud cover

In the total cloud cover analysis, the model background field is replaced by a cloud cover field derived from a temperature-calibrated Meteosat infrared image over its area of coverage. Satellite pixels colder than the model surface temperature by a specified threshold are assumed to be cloud filled. The image resolution is 7km. Counting the cloudy pixels within a model grid-square gives an estimate of the total cover. After use of the imagery,

the cloud cover field is updated from the precipitation analysis by ensuring that the analysed cover is at least as great as the precipitation cover. With the cloud cover field after these two stages acting as a background field, the surface observations are then analysed with a 2-dimensional recursive filter. Analysed cloud cover values of less than 2 oktas are set to zero to give the cloud a well defined edge.

The threshold temperature difference in the satellite diagnosis step was found to require careful tuning. Too high a threshold value can cause problems with relatively warm low cloud over a cold surface. For example, over a cold land surface in winter, the cloud top temperature of a stratocumulus sheet may be similar to that of the ground. With too high a threshold, any cloud correctly present in the model background field may be removed, and if missing in the model, it will not be added. A value of 5K has been found optimal. From comparison with independent sea surface temperature analyses, it appears that the Meteosat infrared data have a 4K cold bias when viewing the surface, most of which is believed to be an atmospheric correction effect. Similar, and possibly even larger, correction effects are estimated by Schmetz (1986). The 5K value is therefore to be interpreted as preventing diagnosis of cloud in clear areas by requiring that the satellite cloud top temperature is at least 1K colder than the surface temperature.

The problem of detecting warm low cloud would be alleviated in daylight hours by including Meteosat visible imagery in the system. This is planned for the future (Jackson 1995). It may also be possible to use visible imagery in the day to derive a more accurate temperature threshold for use with infrared imagery, which would help in the hours of darkness.

(d) Cloud top height - basic approach

Before the infrared image is used for cloud top height assignment, it is corrected for ground radiation effects in areas where the analysed cloud cover is only partial. Then a cloud top height is extracted for each satellite pixel falling in a model grid-square for which the analysed total cloud cover exceeds two oktas. The basic technique involves scanning upwards through the levels of the model background temperature profile until a temperature is reached which matches the satellite temperature. For the treatment of height assignment problems where the basic method is inadequate, see Section 6.

Within the image domain, this cloud top height field is then used to modify the vertical distribution of cloud in the model background field. If the profile of model cloud in a grid-box column unambiguously disagrees with that deduced from the satellite pixels within it, then the model cloud profile is altered by the minimum amount necessary to achieve consistency. Otherwise, the model cloud profile is unaltered. The changes made are based on what is 'seen' by the satellite. No assumptions are made about the cloud at other levels that are hidden. The algorithm to achieve this is described below.

At the bottom level, an initial 'satellite cloud cover' is set equal to the fraction of pixels within the grid-square that are colder than the first-guess temperature (if this does not exceed the analysed total cover). At each level k above, a similar satellite cover N_k is extracted (the fraction of pixels colder than the temperature at that level) and represents the cloud *above* that particular level. The model background cloud profile is then modified. The model cloud fraction at level k , C_k , is reduced where it exceeds the satellite cover for that level; the

revised estimate C'_k is made equal to the satellite cover:

$$C'_k = \min[C_k, N_k] \quad (3)$$

Where the difference in satellite covers between two levels exceeds this revised cloud fraction at the lower of the two levels, a new cloud fraction for the lower level is set to the difference in satellite covers.

$$C''_k = \max[C'_k, N_k - N_{k+1}] \quad (4)$$

The overall cloud top height on the model grid is taken as the highest model level for which there is at least 2 oktas cloud cover in the modified vertical cloud profile.

(e) Cloud base height

Following the analysis of cloud top, surface reports are used to analyse cloud base height. The background field used is the cloud base extracted from the model forecast after it has been updated by the satellite imagery. Cloud base and cloud top are then made to be consistent. Where the cloud base analysis is below about 2.5km, the cloud top height is forced to be at least 150m above the base. Above 2.5km, the satellite-derived cloud top is assumed to be more accurate, so the base is adjusted to be at least 150m below the top. Young and Zack (1994) determine cloud base from observations at the nearest surface station. The horizontal smoothing within MOPS leads to a qualitatively similar result over land, though over the sea, cloud base information comes only from the model forecast.

(f) Multi-level cloud analysis

In this stage, surface observations of cloud, including '8-group' reports of the cover, type and base height of multiple cloud layers, are interpreted as cloud profiles with values on model levels. Interpolated first-guess profiles from the model (improved by satellite imagery as in (d) above) are the starting point for retrieval of these 'observed' profiles. Some semi-empirical rules about the depth and cover of particular kinds of cloud help extract the maximum information from the observations (Wright 1993). Level by level analyses are then carried out, using the retrieved profiles as point data at each level. The total cloud cover, cloud base and cloud top analyses act as constraints. This approach differs from that of Young and Zack (1994), who use surface cloud observations to retrieve humidity profiles based on a statistical analysis of earlier surface data and collocated radiosondes.

Where 8-group reports are available for an observation point, cloud is removed from the levels between the last level processed by a particular 8-group and the level corresponding to the cloud base height of the next 8-group report. The cloud cover to be set in the profile is taken from the report, but may be modified according to cloud type. For example, an upper limit of 4 oktas is imposed for reports of cumulus and cumulonimbus. This cloud cover value is set at all levels from the 8-group cloud base up to the designated cloud top level. The general minimum cloud thickness is 200m, but again this is varied according to cloud type. Cumulus is given a depth of at least 500m and cumulonimbus a minimum depth

of 1000m.

If no 8-groups are included in a particular observation, greater use is made of the cloud information in the main report. The profile interpretation is sectioned into height regimes of fog, low, medium and high cloud. For example, if 'sky obscured' is reported, then full cloud cover is set up to a height of 200m. If the surface report is of medium cloud, then the level with greatest first-guess cloud cover in the height range 2.2-5.6 km has its cloud cover set to the observed total cloud cover. If none is present in the first-guess profile, then the observed value is introduced at the model level lying nearest to the middle of the height range quoted. High cloud is treated similarly.

The final modifications to the cloud analysis seek to extract cloud information from the precipitation analysis. An early attempt along these lines was made by Wolcott and Warner (1981), who employed present weather reports of rain to enforce saturation in initial profiles for a mesoscale model. Young and Zack (1994) use radar data to the same end. In MOPS, absence of rain, or the presence of only light rain, is taken as an indication that the cloud is not glaciated. In this situation, the profile is modified if necessary to ensure that there are two cloud-free layers below the -15°C level. Conversely, where moderate or heavy precipitation has been analysed, 8 oktas cloud cover is set for all levels between and including the 0°C and -15°C levels, allowing glaciation to occur down to the 0°C level. These cloud adjustments are permitted only within the area covered by the radar network. It would be unwise to allow them outside this region where the rainfall analysis is dominated by the model background field.

5. ASSIMILATION OF MOPS CLOUD DATA

(a) *Moisture increments*

The basis of the assimilation technique is the relationship (Figure 10) in the model cloud scheme between grid-box mean relative humidity and cloud fraction (Smith 1990). For assimilation, the 'target' 3-dimensional cloud fraction analysis is converted to a set of relative humidity soundings, which are treated as pseudo-radiosondes with a single grid-point of influence. Where the MOPS cloud fraction is zero and cloud is present in the model, the model humidity is nudged towards the critical threshold for cloud formation (the value of 85% in Figure 10 is used above 900mb, values increase to 91.6% in the bottom model layer). No humidity increments are added if both model and MOPS data are cloud free.

It should be noted that Figure 10 applies only to large-scale, layer, cloud. The operational assimilation of MOPS data has recently incorporated a refinement to account for convective cloud cover co-existing with layer cloud in a grid-box. In the model radiation scheme (Ingram 1993), the layer cloud fraction C_L is interpreted as the fractional cover in the part of the gridbox outside any convective cloud. One may therefore combine C_L and the convective cloud fraction C_{CV} to give a model background value of total cloud C :

$$C = C_{CV} + C_L(1 - C_{CV}) \quad (5)$$

Then, a new target *layer* cloud amount C_L' is calculated which would allow the *total* model

cloud in the grid-box to fit the MOPS data. This is done by setting C in equation (5) to the observed cloud fraction from MOPS, C^{MOPS} , and solving for C_L .

$$C_L' = \frac{C^{MOPS} - C_{CV}}{1 - C_{CV}} \quad (6)$$

This target layer cloud amount is then converted to relative humidity by the curve in Figure 10. Tests show that, in practice, the refinement of allowing for non-zero convective cloud has only a very minor impact. Convective cloud fractions in the mesoscale model do not exceed about 0.4. There are, however, some situations where enough convective cloud exists in the model to fit the MOPS data without any layer cloud contribution, that is when C_{CV} exceeds C^{MOPS} (in which case C_L' is set to zero). In this instance, to try and introduce partial layer cloud by humidity increments would be unrealistic, if in fact convection were the process generating the observed broken cloud cover. This can happen where convection penetrates up into a relatively dry stable layer above an inversion.

Various relationships between relative humidity and cloud fraction have been used in NWP models (see, for example, Campana *et al.* 1994, Carr and Zhao 1994, Dastoor 1994). In some models, the cloudiness is diagnosed as a purely empirical function of humidity, while in others, like the UKMO model, possessing a prognostic total water (vapour plus condensate) variable, the relationship is implicitly determined by the modelling of sub-grid scale condensation processes. The UKMO model's relationship is undoubtedly idealised. Observational studies report cloud at humidities much lower than the critical threshold used here (Walcek 1994). Such studies may influence the development of parametrisation schemes. This, however, is not the issue for *assimilation* of cloud data. It would not be productive to assimilate cloud data into the model in a manner inconsistent with a relationship obeyed by the model cloud scheme, as would happen if some more sophisticated relationship between humidity and cloud were postulated. To obtain a model analysis which fits the cloud observations, the assimilation scheme must respect the model parametrisation as a 'strong constraint'.

The prognostic moisture variable in the UKMO unified model is total water, the sum of humidity mixing ratio, cloud liquid water and cloud ice. After the advection step (and before the assimilation step), total water is partitioned by the cloud scheme into vapour, cloud liquid water and cloud ice amounts. It is natural to enquire whether increments during the assimilation of MOPS cloud data should be made to these condensate amounts as well as to the humidity mixing ratio. Now the partitioning by the cloud scheme results, for cloud fractions less than unity, in cloud liquid and cloud ice mixing ratios which can be expressed as functions of the temperature, pressure and cloud fraction (Smith *et al.* 1992). Therefore, if the assimilation results in a relative humidity consistent with the observed cloud fraction, the cloud water and ice amounts will automatically be in equilibrium with that humidity.

There remains, however, a possibility that the lack of any increments to cloud condensate could delay the convergence to the target relative humidity during assimilation. For example, if relative humidity were increased during the assimilation, without a corresponding increase in cloud condensate, the new total water may, after advection, be partitioned into a slightly lower relative humidity and a slightly greater cloud condensate amount. To test

the importance of this effect, a cloud condensate re-initialisation stage was incorporated at the end of the assimilation step to derive cloud liquid water and cloud ice amounts 'in balance' with the latest relative humidity analysis. Also, an extra call to the model cloud scheme was added immediately before the assimilation scheme to ensure that all moisture fields were 'in balance' on entry. This was necessary because during a model timestep, various physical parametrisation schemes are called between the standard call to the cloud scheme and the assimilation step, and these can disturb the cloud scheme's 'balance' relationships between the moisture variables. The impact of the condensate re-initialisation proved to be negligible, with only insignificant differences in analysed cloud. For cloud cover less than one, therefore, relative humidity increments appear to be sufficient to assimilate cloud observations.

When the cloud fraction reaches unity, there is no longer an equilibrium relationship in the model cloud scheme between cloud condensate and vapour amounts. Instead, the amount of liquid water or ice in the cloud is determined by the relative rates of condensation and precipitation formation. In this situation, it is plausible that information from precipitation observations should become more important. Increments to a prognostic cloud condensate variable derived from precipitation data have been advocated by Carr and Zhao (1994), though they do not restrict their application to the case of full cloud cover. The same authors apply increments from cloud observations to the humidity field but not to the cloud water field, an approach consistent with that taken here for MOPS data.

(b) 'Observation errors' of MOPS cloud data

The assimilation algorithm requires that the 'observation error' be specified, so that the weight of data relative to the model background can be determined. This error should encompass both instrumental and representativeness effects. For MOPS data, the estimation of observational error is less straightforward than for more conventional data types: the data are a combination of different observations with a model background contribution already included, and also the analysis is in terms of cloud fraction, while the assimilation works in terms of relative humidity. In the first operational version, MOPS soundings were empirically given the same weight as radiosondes, but a more physically based approach has since been developed.

To estimate the accuracy of the MOPS cloud fraction analysis at a particular level requires knowledge of the model background error, the errors of all data types influencing the grid-point in question, and an understanding of the errors introduced by the recursive filter analysis technique. Instead, a simpler approach has been adopted. The MOPS analysis of total cloud cover draws closely to the surface reports. So in terms of total cover, a reasonable target for the fit of the model to MOPS data (and hence for the MOPS observation error) is provided by the observation error of surface reports at the model grid-scale. A study of rms total cloud cover differences between neighbouring stations (*Golding*, personal communication) has shown the error of representativeness to be around 1.5 oktas for the mesoscale model grid-box of side 17km (Figure 11). The 'instrumental' error in a surface report of total cloud cover is neglected in comparison with this error of representativeness. Although this error is derived from considering surface data, there would be little merit in attempting to fit MOPS total cloud cover more closely in regions where the data were mainly derived from satellite imagery.

The next step was to move from an observation error for total cloud cover to a relative humidity error at each level in the vertical. This was accomplished by a statistical analysis of radiosondes and collocated 3-hour model forecast profiles, the latter reflecting the error characteristics of MOPS data assimilated 3 hours earlier at $t+0$. Total cloud cover was derived from each by the model's assumption of maximum-random overlap. Profiles which differed in total cover by around 1.5 oktas were extracted and the relative humidity differences as a function of level noted. In this way, a typical profile was built up of the rms relative humidity differences associated with a total cloud cover difference of 1.5 oktas. The method of deriving this error profile does not depend on the absolute accuracy of either the sondes or the 3-hour forecasts, only on the relationship between differences in cloud cover and corresponding differences in relative humidity structure. The MOPS error values obtained were in the range 8-12% for low cloud, 12-20% for medium cloud and 20-24% for high cloud. The errors are dominated by height assignment problems rather than errors in cloud amount at a particular level. For comparison, the assumed errors for radiosonde humidity data range from 8% in the boundary layer to 12% in the upper troposphere.

Some further modification of the MOPS observation errors was carried out for the bottom few model levels. This was to make sure that screen level relative humidity data would be given higher weight near the surface. Unless the surface report is of 'sky obscured', the MOPS cloud fraction at level one near a surface station will be zero and this will tend to keep the relative humidity during assimilation below the critical threshold for cloud formation. In misty conditions, the surface relative humidity may well be higher than this, in which case it would be desirable for the model to fit the surface observation rather than the MOPS data, so that a good visibility diagnosis could be made. For this reason, MOPS data are not assimilated at level one and their observation errors are slightly increased up to level six.

(c) Impact on analyses and forecasts

Before implementation in late 1992, the present mesoscale model underwent an operational trial, when cases drawn from a wide range of synoptic types were run with the full data assimilation system (CONTROL experiments). As an observing system experiment, they were also rerun without MOPS data supplied to the assimilation (noMOPS runs). Objective verification of cloud cover at UK land stations confirmed benefit from MOPS data up to $t+18$ (Figure 12). The higher rms errors of the noMOPS runs are coupled with a greater negative bias in cloud cover. (Cloud cover biases as large as those in Figure 12 are not typical of average model performance, for which the bias is around -0.5 oktas at $t+0$, rising to about +0.5 oktas at $t+18$. Average rms cloud cover errors are close to 2.5 oktas throughout the forecast.)

The benefit from MOPS data is most persistent in anticyclonic cases, when the cloud cover deficiency of the model tends to be greatest. These are often stratocumulus situations, in which model performance has been somewhat erratic. An interesting stratocumulus period, in which the model gave some useful and some very poor predictions, was examined by Ballard and Macpherson (1993). The most serious cause of a deficiency in analysed cloud was identified as a systematic drying of the model due to assimilation of radiosonde relative humidity data. When the radiosonde data were removed, as in the experiments shown in Figure 13, benefits from MOPS cloud data were revealed.

The problems with radiosonde data have been tackled by Lorenc *et al.* (1994). They found that total cloud cover as diagnosed from radiosonde profiles (by the model's cloud algorithms) was systematically less than that reported in the surface observations analysed within MOPS. One reason for this is the limitation of model vertical resolution when it comes to representing thin cloud sheets. When the radiosonde profile is averaged onto model layers, the layer average relative humidity may fall below the model's critical threshold for cloud formation even if the instrument has passed through cloud. A change to the preparation of values on model layers by interpolation of the profile to the layer mid-point was found to alleviate this problem. A second problem is believed to be a dry instrumental bias in cloud of about 3%. A radiosonde bias correction has now been incorporated in the data preparation stage before assimilation. It is applied over the range 80-100%, in which radiosondes are not calibrated (Nash, personal communication). Finally, the forecast error correlation scale for radiosonde humidity data was re-derived from (observation-background) statistics for the mesoscale model. Previous values were based on those for the regional model. The scale has now been reduced from 150km to 105km above, and 85km within, the boundary layer. These three changes have significantly reduced the degradation of cloud analyses and forecasts by radiosonde data.

In most cases with precipitation, the impact from MOPS data is short-lived, no doubt because of the strong dynamical forcing from intruding boundary conditions. The clearest examples of impact from MOPS data in rainfall prediction tend to occur in thundery situations with relatively slack pressure gradients, in which the influence of boundary data is less immediate. A good example is afforded by the forecast on 13th July 1994 (Figure 14), when a band of thunderstorms developed in the Channel during the early morning and moved into south-east England. Benefit lasted for around 9 hours into the forecast. Also in a convective situation, Zack *et al.* (1988) obtained a beneficial impact on precipitation from their moisture analysis which remained throughout a 12-hour forecast.

6. CLOUD TOP HEIGHT ASSIGNMENT PROBLEMS

(a) *Stratocumulus*

In certain situations, large errors can be introduced by the basic method in MOPS of scanning the model temperature profile for a temperature matching the satellite brightness temperature. Cloud top is often associated with a temperature inversion, which can be very marked for persistent stratocumulus sheets. If the inversion is not well resolved by the model, the matched temperature will not correspond to the cloud deck, but to some point much higher where the cloud-free environment temperature has dropped to the value observed by satellite. This problem is reflected in the erroneous placement of the cloud layer in the forecast in Figure 15(b). In the first operational version of MOPS, which was an interactive system, a forecaster could easily detect such a problem in the automatic cloud top height analysis and modify this field interactively to set sensible cloud tops, using available radiosonde ascents as a guide.

To provide a more reliable automatic method of height assignment, especially in stratocumulus situations, a second algorithm was developed. It begins with an idealised vertical profile of temperature and humidity through a stratocumulus layer (Figure 16).

Above the cloud the air is warm and dry. At the cloud top there is a marked inversion; the cloud top temperature is that at the base of the inversion. Within the cloud the air is well mixed by turbulence and has a constant wet bulb potential temperature (θ_w). Beneath the cloud the air is also well mixed with the same θ_w as in the cloudy layer, but the relative humidity decreases downwards. The temperature lapse rate approximates the dry adiabatic value and the humidity mixing ratio is constant.

The role of this idealised profile in determining cloud top height is illustrated by Figure 17. At a level near the surface, the model background temperature and dew point are selected. Starting from this reference level, the condensation level (Normand's point) is located by assuming adiabatic cooling from the reference level until saturation. This level is taken as cloud base. From this point the air is allowed to cool at the saturated adiabatic lapse rate until it reaches the temperature, T_{sat} , of the satellite-observed cloud top. Using the temperatures and dew points at the cloud top, cloud base and reference level, a layer thickness is calculated from the hydrostatic equation. The height of the model reference level above ground is then added to the thickness to obtain cloud top height. Cloud top heights derived from the idealised profile are used to modify the model cloud profile in a similar way to those obtained by scanning the model temperature profile.

The idealised profile algorithm was validated in several stratocumulus cases by Hand (1993) and Wright, (1993). The first task was to establish the best reference level from which to choose the model temperature and dew point. Various levels were tested and the cloud top height fields were verified against radiosonde ascents. The optimal reference level proved to be around 180m. This gave rms cloud top height errors of around 300m and a mean error of about 10m. To put these results in perspective, most of the cloud top heights for verification were in the region of 600-1200m and the average thickness of model layers in this height range is approximately 200m. The idealised profile scheme compared very favourably with the one that simply matches T_{sat} to model temperature profiles, which returned an rms error of about 900m and a mean error of around 400m. Implementation of the idealised profile technique permitted full automation of MOPS, with a beneficial saving of forecasters' time. An example of the method's value is shown in Figure 15(c).

Although developed with stratocumulus in mind, the idealised profile algorithm can be applied more widely. It has been found to yield sensible cloud top heights in regions where thick multiple layers are present as opposed to just low stratiform cloud. It does encounter a problem when the derived cloud base temperature is lower than the satellite cloud top temperature, as may happen if the model reference level θ_w is too cold, or in regions of very broken cloud over a warm surface. In this situation it is better to select the technique of scanning the background temperature profile for a value matching T_{sat} . The same action is taken if the model temperature at the reference level is less than T_{sat} . Also, it would not be appropriate to analyse cirrus heights via the idealised profile, so its application is restricted to pixels with T_{sat} greater than $-20\text{ }^{\circ}\text{C}$. The temperature profile scanning method is applied above this level (around 5.5km).

As mentioned above, in the earlier interactive version of MOPS, forecasters took guidance on cloud top height from radiosondes, but these do not enter the above automatic algorithm except for 'calibration' of the scheme's tunable parameters. This may be considered a weakness. However, radiosonde data are sparsely distributed and the automatic algorithm

must derive cloud top heights over the sea far from the nearest sounding. This problem has been recognised in the operational cloud top height scheme of the Italian Meteorological Service (Pagano *et al.* 1994), in which temperature soundings from a polar orbiting satellite are used where radiosondes are not available. The satellite soundings are helpful for medium and high cloud, but are not informative about the low level temperature structure typical of stratocumulus. The Italian cloud top product is used mainly as a qualitative nowcasting tool for aviation. Assimilation into a mesoscale model places more stringent accuracy requirements on the height assignment of low cloud.

(b) *Thin high cloud*

Some relatively long-lived forecast impacts from MOPS data have been noted in which spurious rainfall areas have been generated by the triggering of medium-level instability in the model. The analysis may show only a small area of convective rain, perhaps some way ahead of a frontal band, but this feature may develop and last for 12-15 hours into the forecast, occasionally becoming involved with the frontal band in a quite unrealistic manner. Occasionally, the spurious rain area in the analysis is extensive, as in the example shown in Figure 18(b). Investigation of the MOPS analysis process for this case showed that omission of the Meteosat imagery led to removal of most of the spurious rain, as can be seen from the noSAT run in Figure 18(c). The main effect of the satellite imagery in the area of spurious rain was found to be removal of high cloud at 300mb from the model background field, and insertion of medium level cloud around 725mb. This process took place over a 9-hour period prior to data time at 6 UTC. It is believed that during this time, in the area affected by spurious rain, the satellite was observing thin cirrus from an older frontal system, through which the surface was 'visible', thus giving much too warm a cloud top temperature. This resulted in a height assignment for the observed cloud which was far too low.

This interpretation of the problem has now been formulated as a change to the MOPS algorithm for use of infrared imagery. At grid-points where the model background field contains 'high' cloud, the satellite image is not used to modify the *height* of cloud layers in the model profile. Cloud *amounts* in the profile are still changed to reflect the total cloud cover diagnosed from the satellite, which is not in doubt. This 'quality control' strategy for use of imagery is very successful in eliminating most of the spurious rain in the case shown in Figure 18 (see the qcSAT run in frame (d)). The area over which the model high cloud has restricted use of the imagery can be seen in Figure 19 and compared with the corresponding infrared image. The same approach proved beneficial in several other test cases with spurious rain and was implemented operationally in April 1995. In another two cases in which thunderstorms *did* develop in both the real atmosphere and the model, the effect of revised imagery quality control based on model high cloud did not give any systematic change in forecast accuracy.

Of course, the reliance of the decision on the accuracy of high cloud in the model's 3-hour forecast is not ideal, but the precaution of not using some of the satellite information when it may be suspect is easier than trying to detect, and assign a height to, thin cirrus in the image itself. In cases where cirrus is present in the model and cirrus would be assigned from the imagery, there is already little to be gained from the imagery, apart from a correction to the amount of high cloud. In cases where the model has cirrus, but the imagery shows no cloud, the erroneous model cloud will still be removed by the MOPS total cloud

cover step. For a more sophisticated solution to the problem, one may look to operational methods for the generation of cloud motion winds from Meteosat infrared data (Schmetz *et al.* 1993), which include a semi-transparency correction for the height assignment of high cloud. Simultaneous water vapour imagery is needed, along with radiation model calculations based on temperature and humidity profiles from an NWP model. Such techniques may be adopted within MOPS in future.

7. CURRENT DEVELOPMENTS AND PLANS

The MOPS cloud analysis contains a precipitation rate analysis, which we have now begun to exploit as a data source in its own right, rather than just as a constraint on the 3-D cloud analysis. The first application has been for verification of precipitation analyses and forecasts from the mesoscale model. Previously, objective verification of model precipitation has relied on the relatively sparse surface network and focused on 6-hourly accumulations. The MOPS analysis gives much wider coverage and is smoothed to a scale close to the effective resolution of the model. It is useful for verifying instantaneous model fields. Categorical measures, such as the model's accuracy of rain/no rain prediction, are helpful in validating model changes.

For assimilation purposes, the precipitation analysis has recently been incorporated into a surface hydrology correction scheme (Jones and Macpherson 1995). This scheme derives increments to soil moisture content and snow depth based on differences between model rain rates and those in the MOPS analysis. The next application will exploit the rainfall data more directly within the atmospheric model. It is planned to achieve this by 'latent heat nudging', a technique which has proven potential to improve short-period precipitation forecasts, as demonstrated for example by Wang and Warner (1988) and Manobianco *et al.* (1994).

The benefit of surface humidity data for fog prediction was discussed in Section 3. To help improve the model's handling of visibilities in the 1-5km range, it is planned to assimilate surface visibility reports. Along with the collocated humidity measurement, these will be used to derive an increment to the aerosol concentration variable that is carried as a tracer in the model. Visibility forecasts at sea may be improved by a better sea surface temperature (SST) analysis. The rather sparse *in situ* data available to the current operational mesoscale SST analysis will be augmented by high density satellite (AVHRR) measurements in the near future (Jones 1994).

Doppler radars are a relatively new data source in the UK with scope for describing mesoscale detail in the wind field where precipitation is observed. There are currently two radars in the UK network with Doppler capability, at Cobbacombe Cross and Clee Hill. Brown (1994) has compared Doppler derived radial wind components with collocated radiosondes and found rms errors in the radial winds of less than 2ms^{-1} , for measurements averaged over several square kilometres. The data assimilation scheme can easily be adapted to assimilate such single component wind data, and impact studies are planned.

Looking further ahead, the mesoscale assimilation system will be run on an hourly cycle (Maycock 1995) as part of the 'Nimrod' nowcasting system mentioned in Section 4(a). The

Nimrod project also includes developments in rainfall analysis which should lead to improved quality in the data passed to the latent heat nudging scheme for precipitation assimilation.

Finally, as already mentioned, the overall approach to data assimilation in the Meteorological Office is moving towards that of four-dimensional variational analysis. It is envisaged first that a three-dimensional variational scheme will replace the current 'Analysis Correction' Scheme, then development of an operationally feasible four-dimensional system will be tackled. For the mesoscale model, continuous nudging of cloud and rainfall data is likely still to play a significant role alongside the three-dimensional variational assimilation of more conventional data. Four-dimensional variational assimilation of the data sources described in this paper will be a very challenging, but potentially rewarding project.

ACKNOWLEDGEMENTS

B.W. Golding has overseen the development of the operational mesoscale forecast model and data assimilation system. S. P. Ballard and R.N.B. Smith have led the effort to improve the forecast model, with contributions from P.A. Clark, S.D. Jackson and S.A. Woltering. R.W. Robinson and forecasters of the Central Forecasting Office have assessed the quality of analyses and forecasts. Regular objective measures of model performance have been provided by the verification group in Central Forecasting Systems under Dr R.A. Bromley.

REFERENCES

Internal reports of the UK Meteorological Office are available from the National Meteorological Library, Meteorological Office, London Road, Bracknell, Berkshire RG12 2SZ.

Ballard, S.P., Robinson, R.W., Barnes, R.T.H., Jackson, S.D. and Woltering, S.A. 1993: Development and performance of the new mesoscale model. UK Meteorological Office, Forecasting Research Division, Technical Report No. 40.

Ballard, S.P. and Macpherson, B. 1993: Operational performance of mesoscale and LAM models in prediction of stratocumulus. UK Meteorological Office, Forecasting Research Division, Technical Report No. 56.

Bell, R.S., Lorenc, A.C., Macpherson, B., Swinbank, R. and Andrews, P. 1993: The Analysis Correction Data Assimilation Scheme. UK Meteorological Office, Unified Model Documentation Paper No 30.

Brown, C. 1994: Accuracy of wind measurements from an SPS Doppler weather radar. UK Meteorological Office, Forecasting Research Division, Technical Report No. 105.

Carr, F.H. and Zhao, Q. 1994: The initialization of cloud water/ice in NMC's ETA model. Pp 303-305 in Preprints, 10th AMS Conf. Numer. Weather Predict., 18-22 July., 1994, Portland, Oregon.

Chouinard, C., Mailhot, J., Mitchell, H.L., Staniforth, A. and Rogue, R. 1994: The Canadian regional data assimilation system: operational and research applications. *Mon. Weather Rev.*, **122**, 1306-1325.

Clark, P.A., Jackson, S.D., Macpherson, B., Maycock, A.J., Robinson, R.W., Smith, R.N.B., Woltering, S.A. and Wright, B.J. 1994: Developments of the mesoscale model during 1993. UK Meteorological Office, Forecasting Research Division, Technical Report No. 91.

Cullen, M.J.P., 1991: The unified forecast/climate model. UK Meteorological Office, Short-range Forecasting Research Division Scientific Paper No.1.

Daley, R. 1991: Section 4.3 in Atmospheric Data Analysis, Cambridge University Press, 457pp.

Dastoor, A.P., 1994: Cloudiness parametrization and verification in a large-scale atmospheric model. *Tellus.*, **46A**, 615-634.

Garand, L. 1993: A pattern recognition technique for retrieving humidity profiles from Meteosat or GOES imagery. *J. Appl. Meteorol.*, **32**, 1592-1607.

Golding, B.W., 1990: The Meteorological Office mesoscale model. *Meteorol. Mag.*, **119**, 81-86.

Hand, W.H., 1993: A method of improving the analysis of cloud top height for the new mesoscale model. UK Meteorological Office, Forecasting Research Division, Technical Report No. 53.

Hayden, C.M. and Purser, R.J. 1988: Three-dimensional recursive filter objective analysis of meteorological fields. Pp 185-190 in Preprints, 8th AMS Conf. Numer. Weather Predict., 22-26 Feb., 1988, Baltimore, Md.

Ingram, W.J. 1993: Radiation. UK Meteorological Office, Unified Model Documentation Paper No 23.

Jackson, P. 1995: thresholding methods for the identification of cloud in Meteosat imagery. UK Meteorological Office, Forecasting Research Division, Technical Report No. 154.

Jones, C.P. 1994: Report on quality and potential use of Autosat-2 SST data. UK Meteorological Office, Forecasting Research Division, Technical Report No. 131.

Jones, C.D. and Macpherson, B. 1995: A hydrology correction scheme for the mesoscale model using observed precipitation rates. UK Meteorological Office, Forecasting Research Division, Technical Report No. 151.

Krishnamurti, T.N., Xue, J., Bedi, H.S., Ingles, K. and Oosterhof, D. 1991: Physical initialization for numerical weather prediction over the tropics. *Tellus.*, **43AB**, 53-81.

Krishnamurti, T.N., Rohaly, G. and Bedi, H.S. 1994: On the improvement of precipitation forecast skill from physical initialization. *Tellus.*, **46A**, 598-614.

Lorenc, A.C. 1986: Analysis methods for numerical weather prediction. *Q.J.R. Meteorol. Soc.*, **112**, 1177-1194.

Lorenc, A.C. 1994: Development of an operational variational assimilation scheme. UK Meteorological Office, Forecasting Research Division, Technical Report No. 116.

Lorenc, A.C., Barker, D., Bell, R.S., Macpherson, B. and Maycock, A.J. 1994: On the use of radiosonde humidity observations in mid-latitude NWP. UK Meteorological Office, Forecasting Research Division, Scientific Paper No. 28.

Lorenc, A.C., Bell, R.S. and Macpherson, B. 1991: The Meteorological Office analysis correction data assimilation scheme. *Q.J.R. Meteorol. Soc.*, **117**, 59-89.

Macpherson, B., Wright, B.J. and Maycock, A.J. 1993: Performance of the data assimilation scheme in the operational trial of the new mesoscale model. UK Meteorological Office, Forecasting Research Division, Technical Report No. 39.

- Manobianco, J., Koch, S.E., Karyampudi, V.M. and Negri, A.J. 1994: The impact of assimilating satellite-derived precipitation rates on numerical simulations of the ERICA IOP4 cyclone. *Mon. Weather Rev.*, **122**, 341-365.
- Maycock, A.J. 1993: Development of the surface data assimilation scheme for the new mesoscale model. UK Meteorological Office, Forecasting Research Division, Technical Report No. 43.
- Maycock, A.J. 1995: Report on the performance of an hourly data assimilation cycle for the mesoscale model. UK Meteorological Office, Forecasting Research Division, Technical Report No. 155.
- Mills, G.A. and Davidson, N.E. 1987: Tropospheric moisture profiles from IR satellite imagery: system description and analysis/forecast impact. *Australian Meteorol. Mag.* **35**, 109-118.
- Pagano, P., De Leonibus, L. and Travaglioni, F. 1994: The operational use of cloud top height maps derived from Meteosat IR images and using TOVS data. Proc. 10th Meteosat Scientific Users' Conf., Cascais, Portugal, 5th-9th Sept. 1994, pp117-126.
- Puri, K. and Miller, M.J. 1990: The use of satellite data in the specification of convective heating for diabatic initialization and moisture adjustment in numerical weather prediction models. *Mon. Weather Rev.*, **118**, 67-93.
- Richards, N.S. and Bell, R.S. 1994: Assimilation of AVHRR cloud top temperature - preliminary experiments. UK Meteorological Office, Forecasting Research Division, Technical Report No. 118.
- Schmetz, J. 1986: An atmospheric correction scheme for operational application to Meteosat infrared measurements. *E.S.A. Journal*, **10**, 145-159.
- Schmetz, J., Holmlund, K., Hoffman, J., Strauss, B., Mason, B., Gaertner, V., Koch, A. and Van de Berg, L. 1993: Operational cloud-motion winds from Meteosat infrared images. *J. Appl. Meteorol.*, **32**, 1206-1225.
- Segami, A., 1992: Spin-up problems of the UKMO mesoscale model and moisture nudging experiments. UK Meteorological Office, Short-range Forecasting Research Division, Technical Report No. 9.
- Smith, R.N.B. 1990: A scheme for predicting layer clouds and their water content in a general circulation model. *Q.J.R. Meteorol. Soc.*, **116**, 435-460.
- Smith, R.N.B., Gregory, D. and Wilson, C.A. 1992: Calculation of saturated specific humidity and large-scale cloud. UK Meteorological Office, Unified Model Documentation Paper No 29.
- Walcek, C.J. 1994: Cloud cover and its relationship to relative humidity during a springtime midlatitude cyclone. *Mon. Weather Rev.*, **122**, 1021-1035.

Wang, W. and Warner, T.T. 1988: Use of four-dimensional data assimilation by Newtonian relaxation and latent heat forcing to improve a mesoscale-model precipitation forecast: A case study. *Mon. Weather Rev.*, **116**, 2593-2613.

Wolcott, S.W. and Warner, T.T. 1981: A humidity initialization utilizing surface and satellite data. *Mon. Weather Rev.*, **109**, 1989-1998.

Wright, B.J., 1993: The Moisture Observation Pre-processing System (MOPS). UK Meteorological Office, Forecasting Research Division, Technical Report No. 38.

Wright, B.J., 1993: Evaluation of the automated version of the Moisture Observation Pre-processing System (AutoMOPS). UK Meteorological Office, Forecasting Research Division, Technical Report No. 79.

Wright, B.J., and Golding, B.W. 1990: The Interactive Mesoscale Initialization. *Meteorol. Mag.*, **119**, 234- 244.

Young, S.H. and Zack, J.W. 1994: The use of non-standard data to improve the initialisation of relative humidity data in mesoscale models. Pp 326-327 in Preprints, 10th AMS Conf. Numer. Weather Predict., 18-22 July., 1994, Portland, Oregon.

Zack, J.W., Karyampudi, V.M., Mattocks, C.A. and Coats, G.D. 1988: Meso-beta scale simulations of convective cloud systems over Florida utilizing synthetic data derived from GOES satellite imagery. Pp 293-300 in Preprints, 8th AMS Conf. Numer. Weather Predict., 22-26 Feb., 1988, Baltimore, Md.

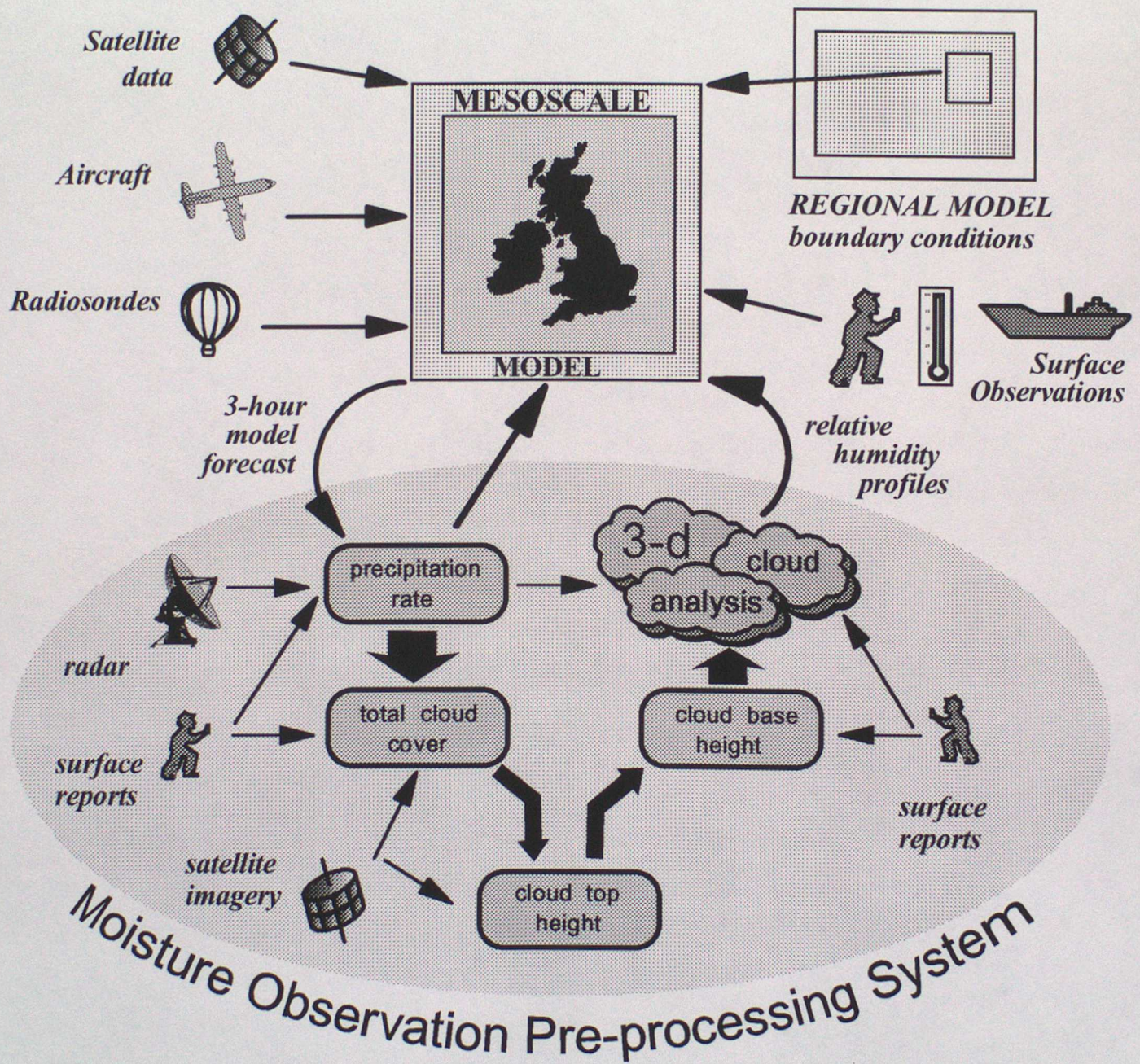


Figure 1: Schematic diagram of the mesoscale data assimilation scheme

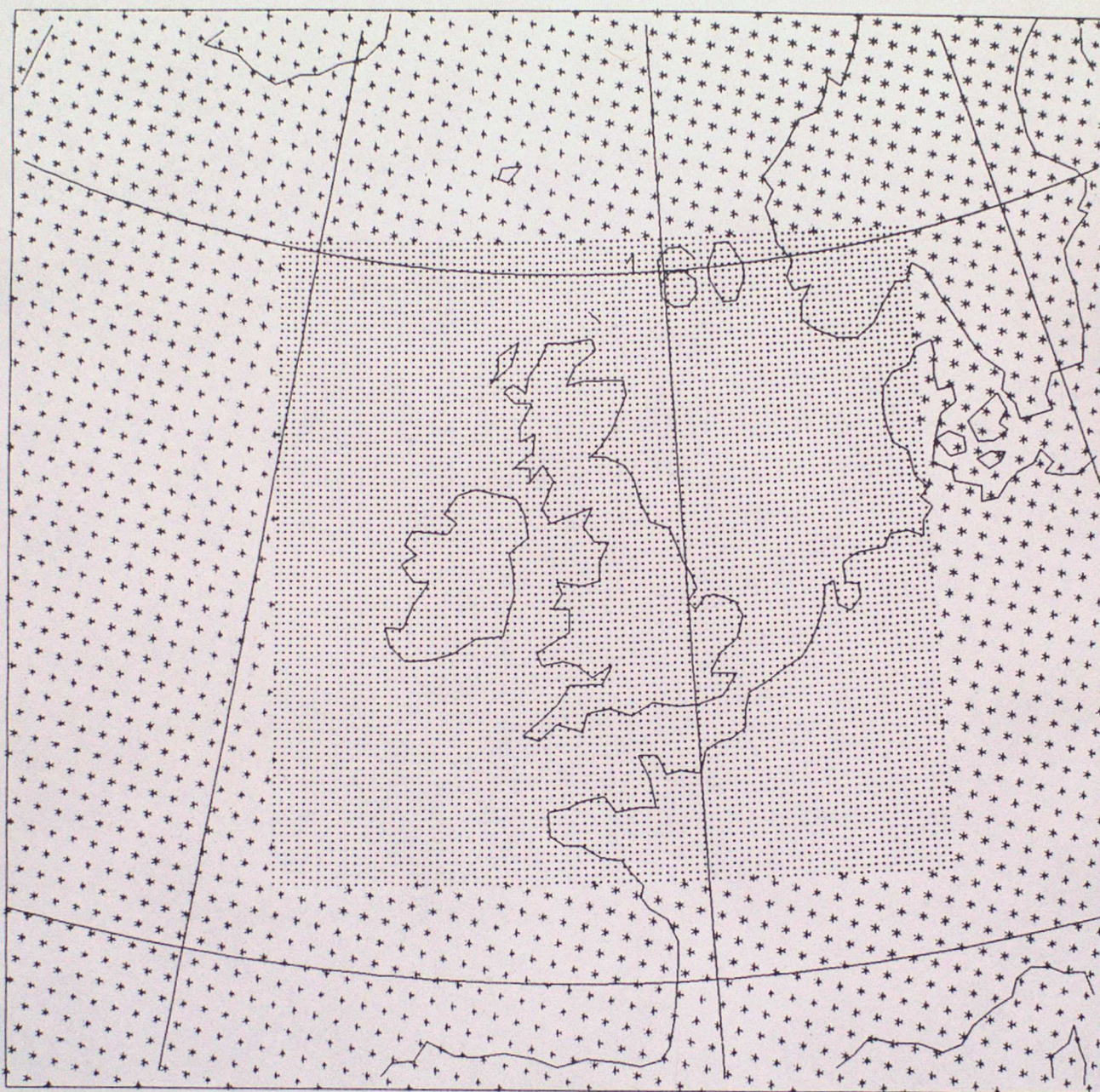


Figure 2: Mesoscale model grid with surrounding grid of the regional model.

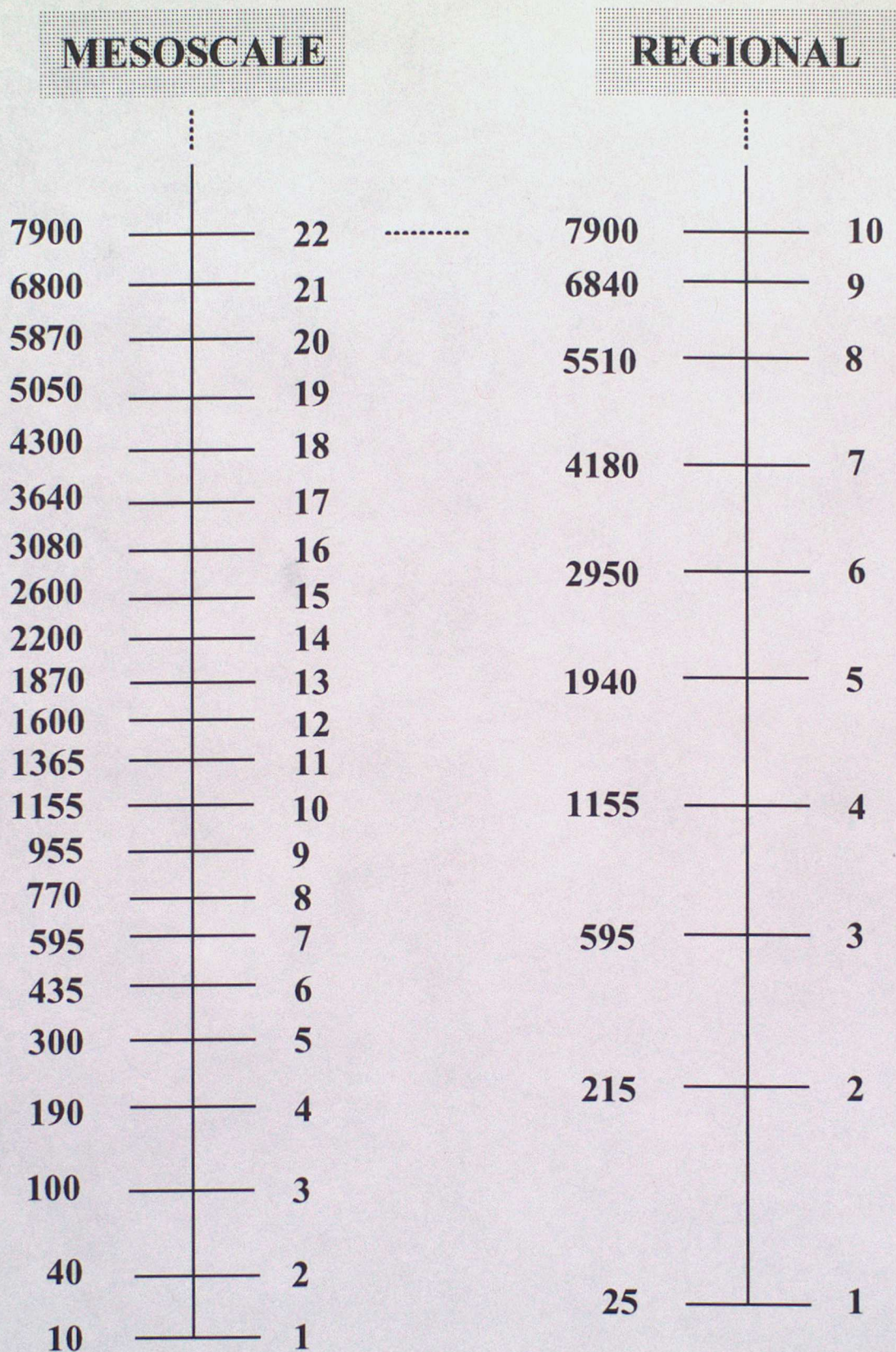
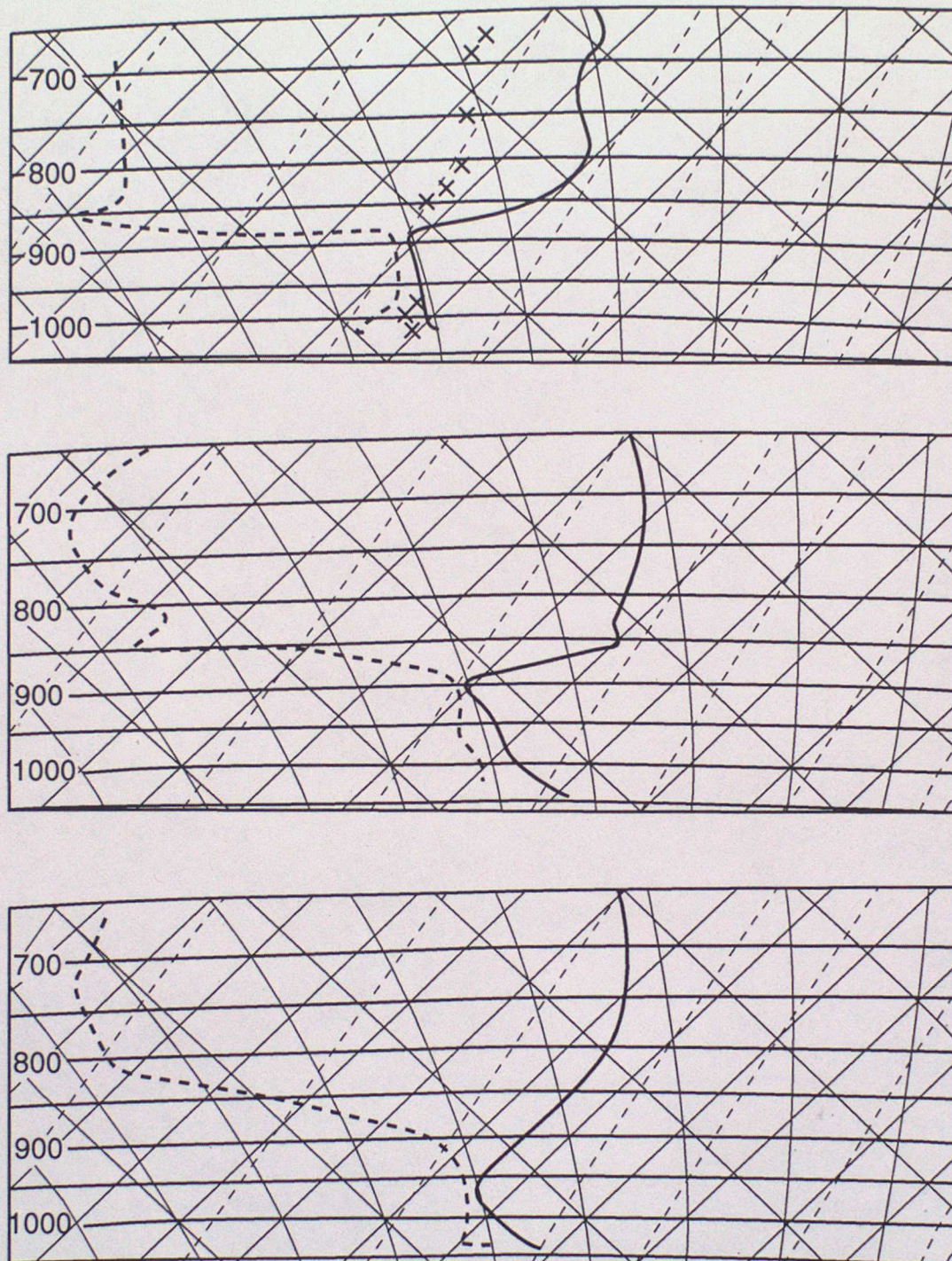


Figure 3: Approximate heights in metres of mesoscale model levels below 8km, with regional model levels for comparison. The mesoscale model has 31 levels and the regional model has 19. Levels 23-31 in the mesoscale version and levels 11-19 in the regional model (not shown) are at identical heights.



Figure 4: Mesoscale model orographic height, with contours at 100m intervals. The coastline is indicated by the 1m contour.



94/1060

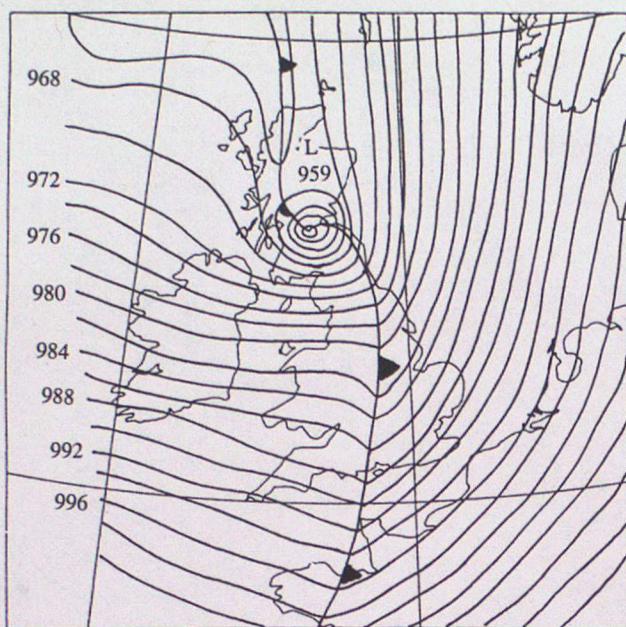
Figure 5: The impact on forecast temperature and moisture profiles of increased vertical resolution in the mesoscale model and in radiosondes assimilated by it.

top : observed ascent from Camborne at 12 UTC, 4th December 1991.

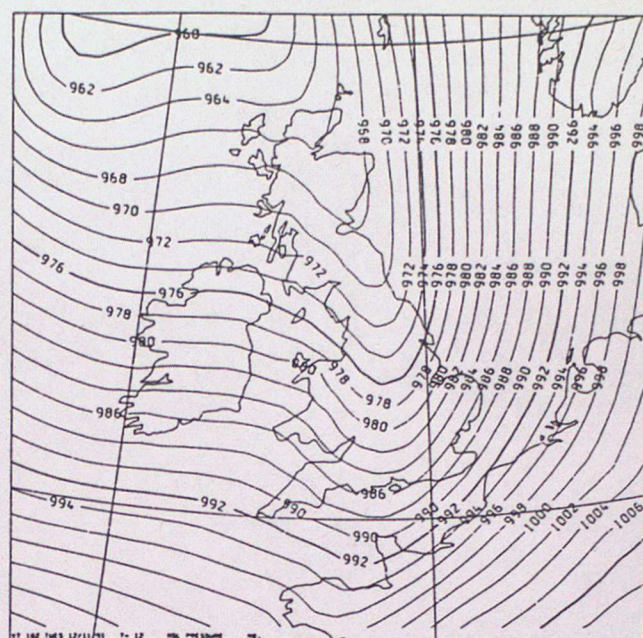
middle : 12-hour mesoscale model forecast from data time 00 UTC.

bottom: as middle panel, but from regional model with coarser vertical resolution.

Note the difference in detail at the inversion and cloud base.



(a)

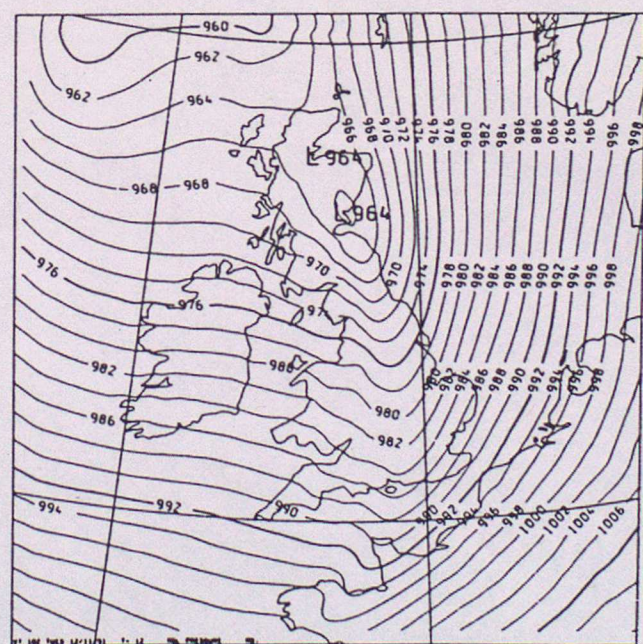


(b)

Figure 6: Impact of model resolution and data differences on forecast of a small scale depression.

- (a) Hand-drawn surface pressure analysis for 18 UTC 12th November 1991.
- (b) 6-hour *regional* model forecast from 12 UTC data time.
- (c) As (b), but from *mesoscale* model, with extra surface data not assimilated in regional model.

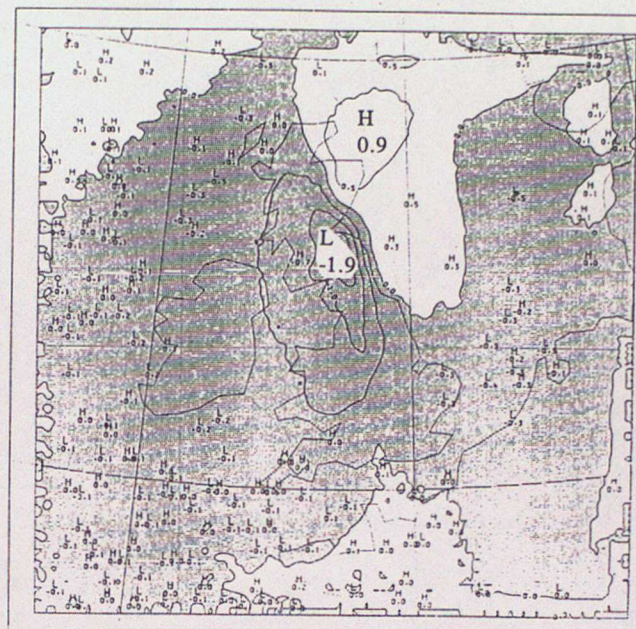
(continued on next page)



(c)



(d)

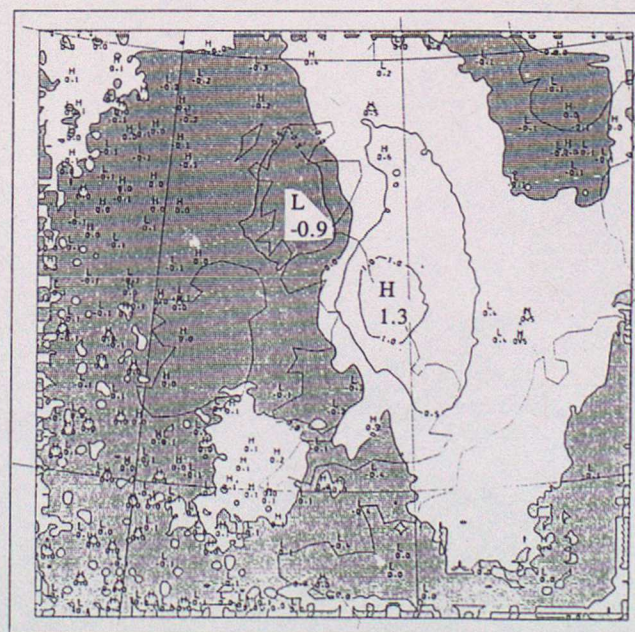


(e)

Figure 6: (contd) Surface pressure difference charts for 6-hour forecasts valid at 18 UTC on 12th November 1991. Contour interval is 0.5mb in each. Negative differences are shaded.

- (d) impact from model resolution: mesoscale model - regional model, with same data supplied to each.
- (e) impact from assimilation of 10m wind data in mesoscale model.
- (f) impact of surface data frequency in mesoscale model:

run with hourly data -
run with 3-hourly data.



(f)

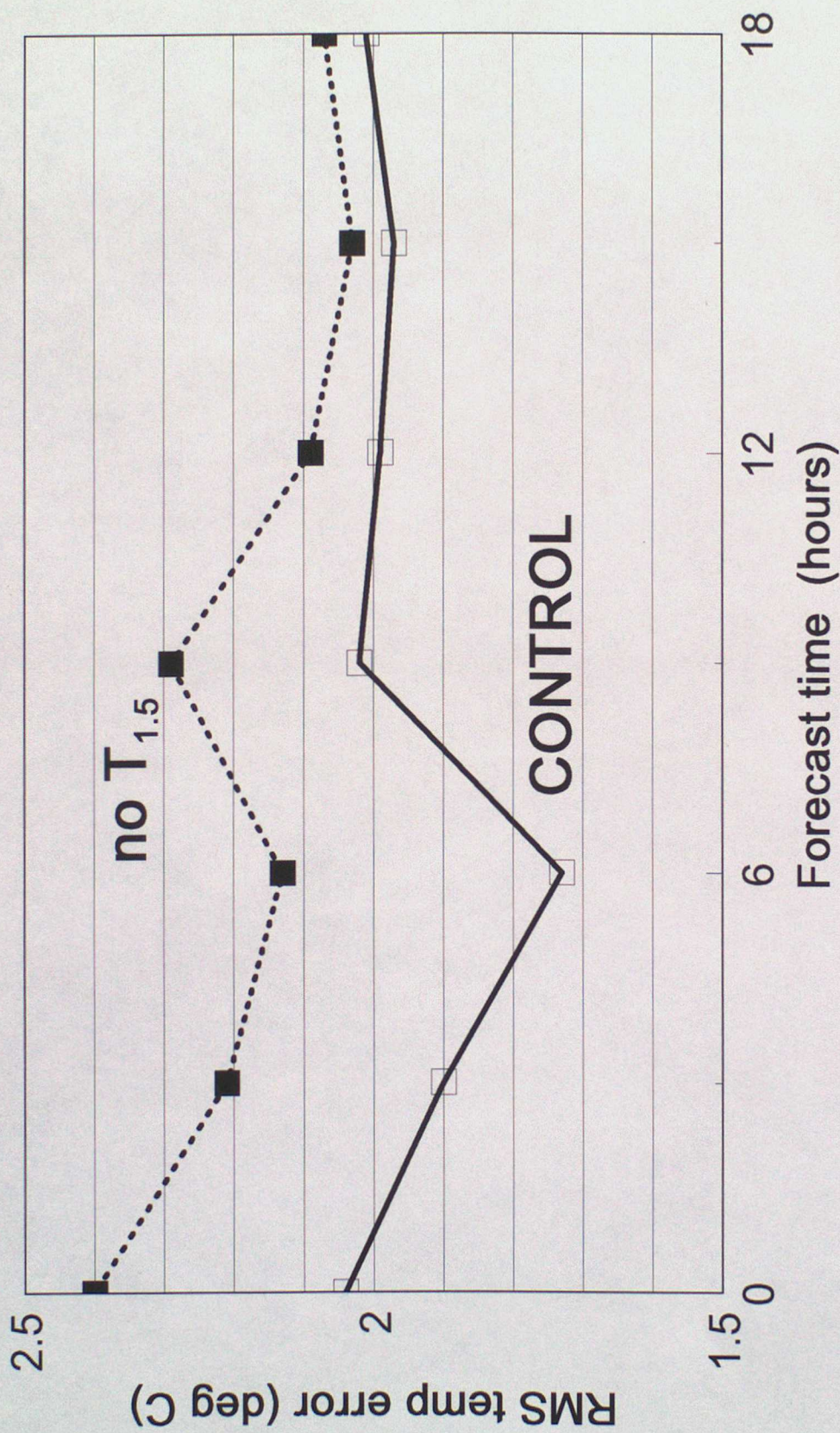


Figure 7: Impact on rms screen temperature errors from assimilation of screen temperature observations. Results are shown for 9 trial cases where the data were included (CONTROL) and omitted (no $T_{1.5}$)

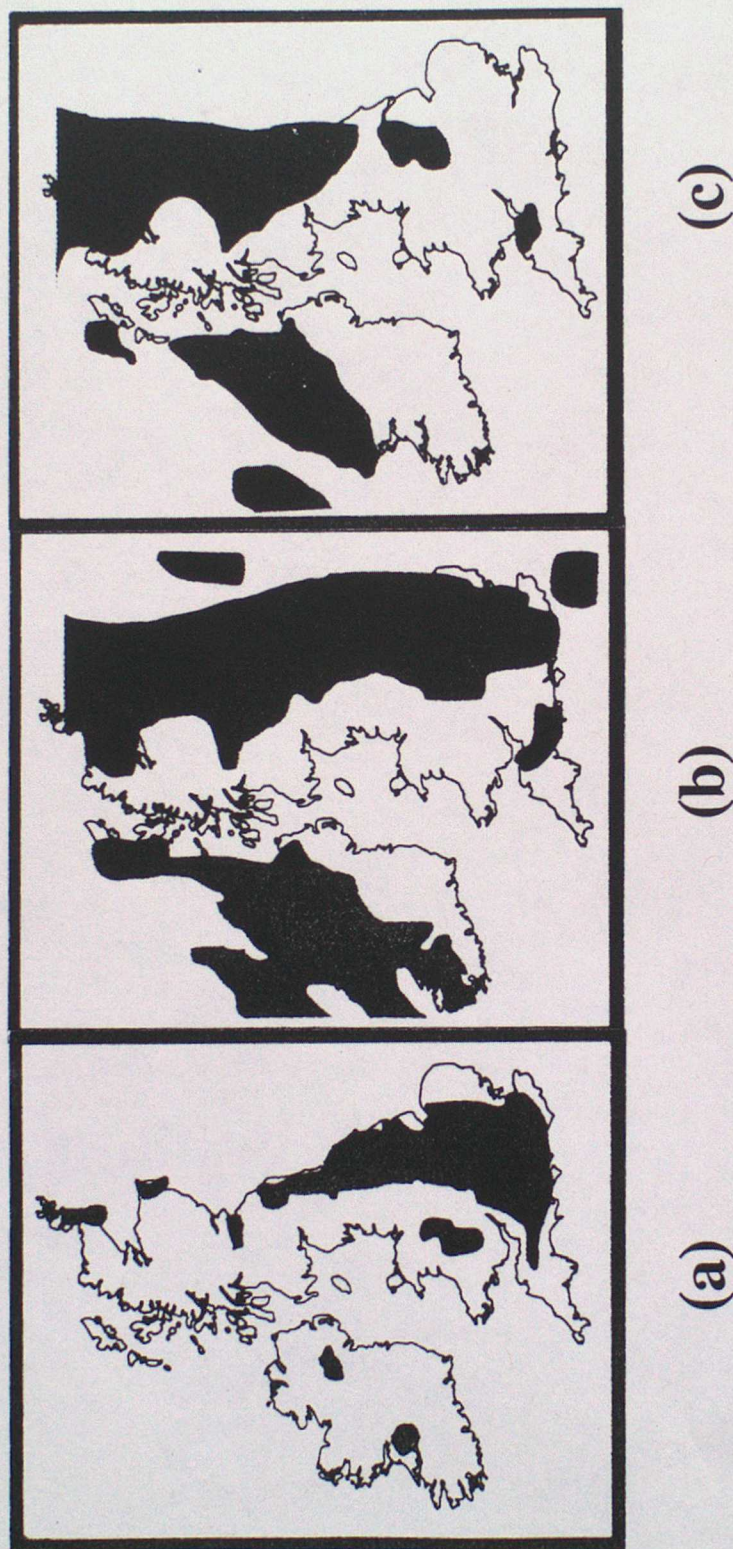


Figure 8: A case showing benefit from assimilation of screen level relative humidity data.

- (a) Observed areas of fog at 6 UTC 30th April 1993.
- (b) 6-hour mesoscale model forecast from 0 UTC data time, with area of 'fog probability' > 20% shaded.
- (c) As (b), but from an analysis *omitting* screen level relative humidity data.

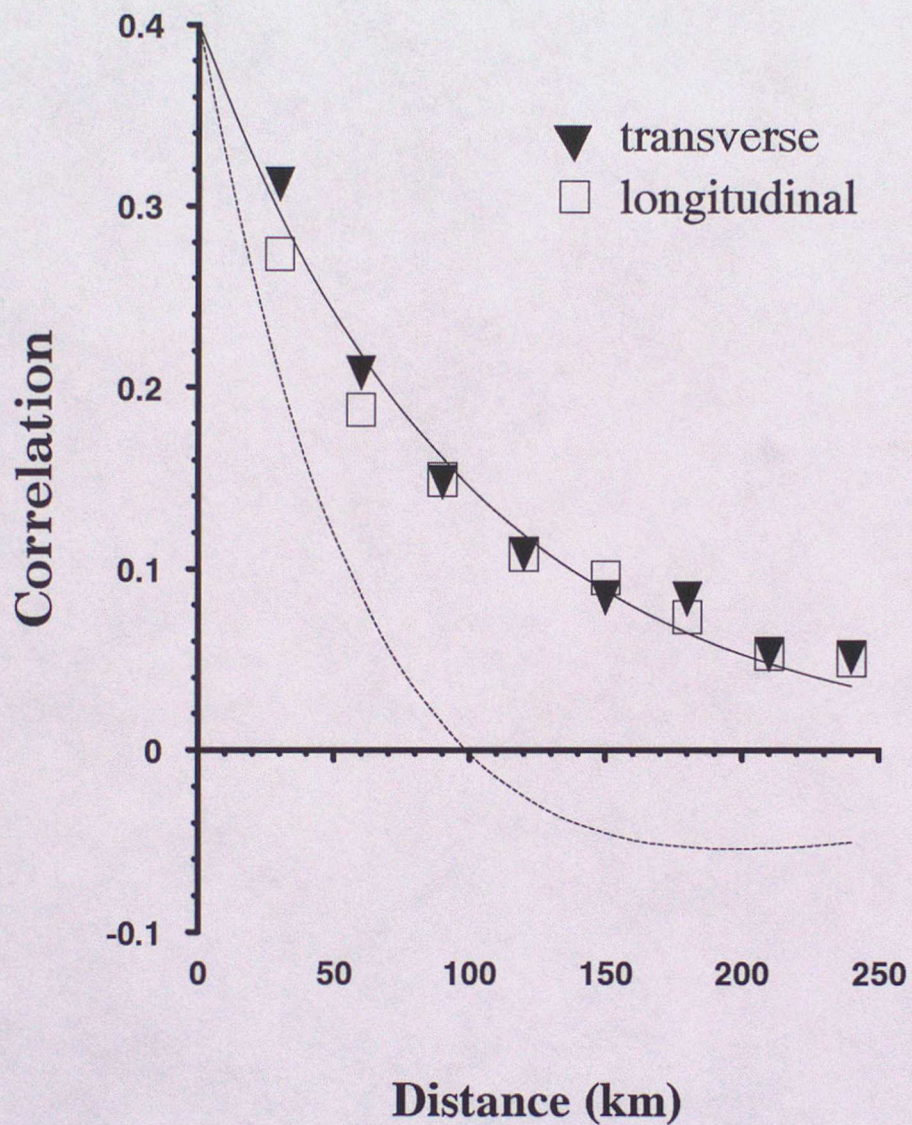


Figure 9: Horizontal correlations of mesoscale model background errors in 10m wind. The plotted points were derived from a 3-month analysis of (observation-background) differences for station separations grouped in 30km bins. Longitudinal and transverse correlations are plotted. The solid line is the best-fit curve of the form in equation (2a), the dashed line is the corresponding curve of form (2b) with $\sigma = 1$.

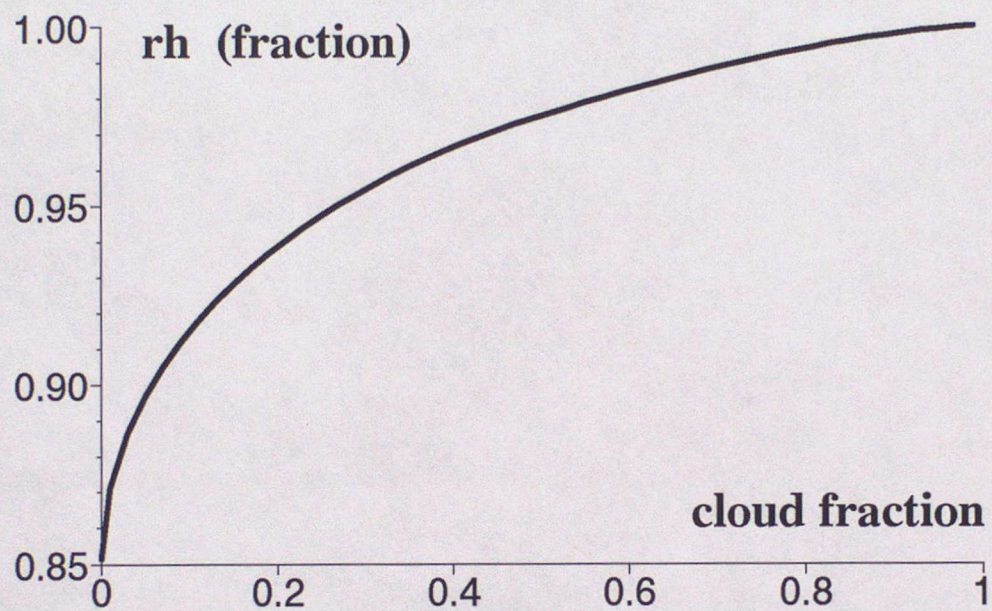


Figure 10: Relationship between grid-box mean relative humidity (rh) and cloud fraction in the UKMO unified model. The critical threshold for cloud formation is $rh=0.85$.

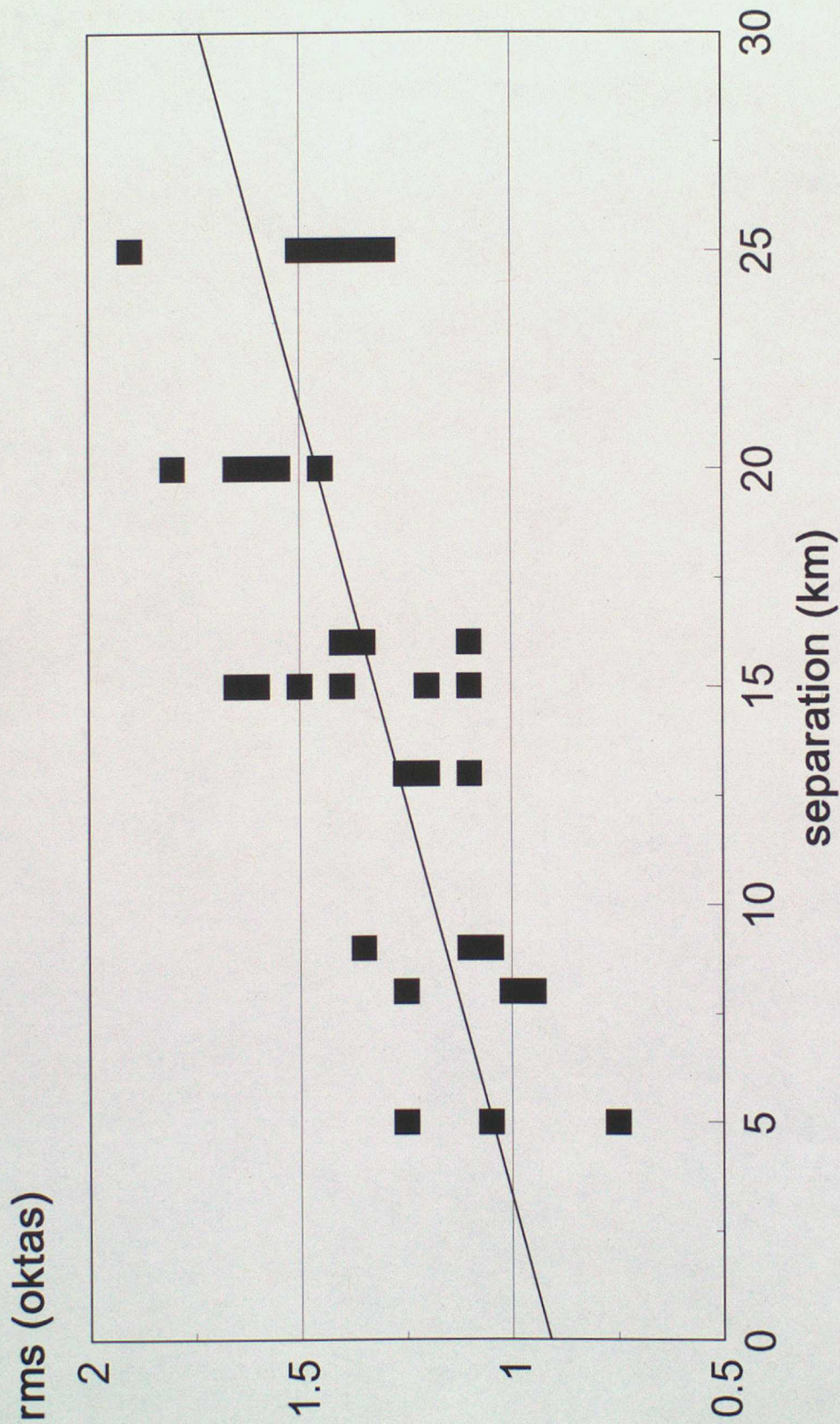


Figure 11: Rms total cloud cover differences as a function of separation for nearby station pairs in the UK. Each point plotted represents an average of one month's data from either December 1991, May 1992 or August 1992.

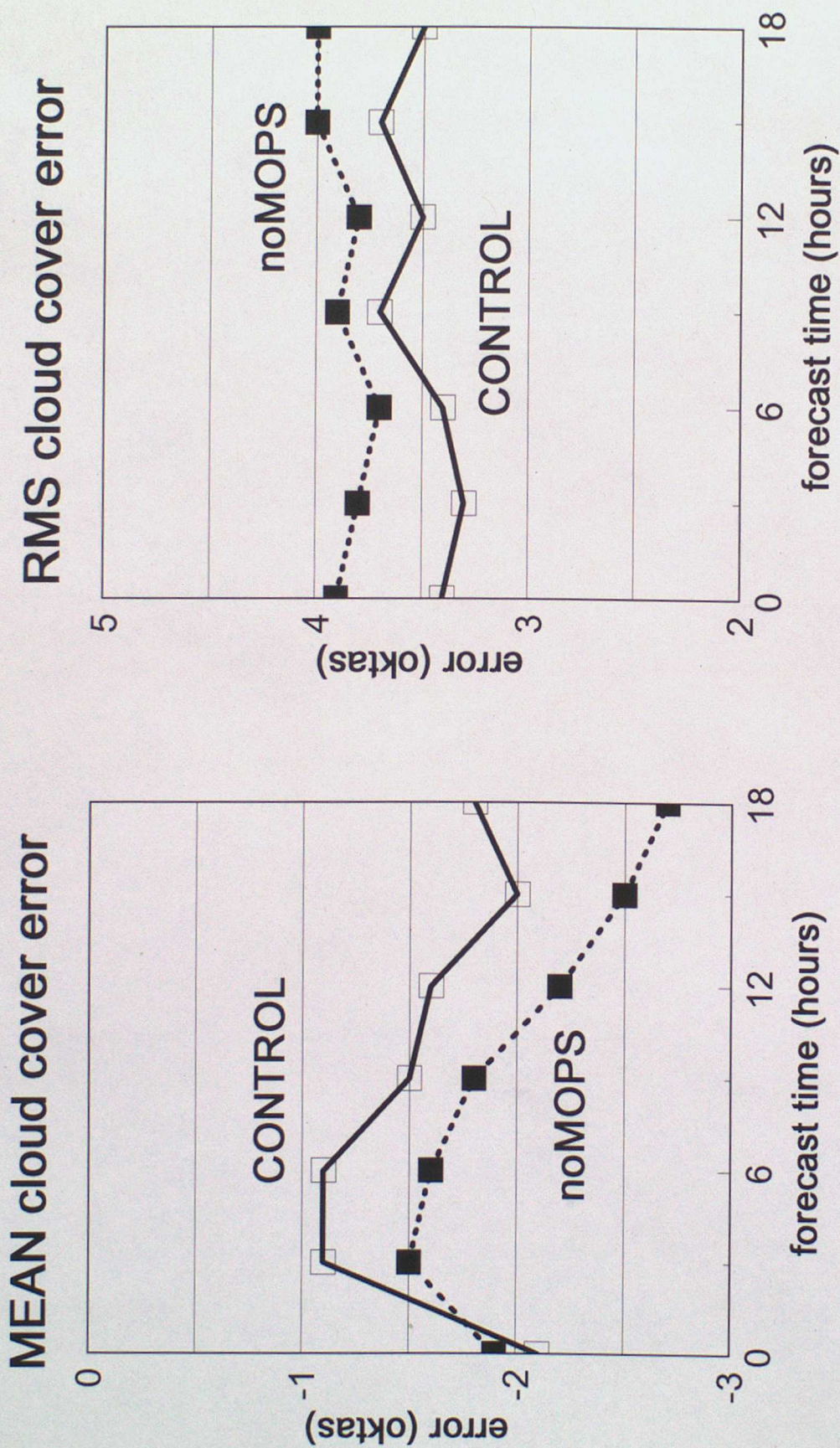


Figure 12: Verification of total cloud cover for 5 cases from mesoscale model trials. In the CONTROL runs, MOPS cloud data were assimilated. In the noMOPS runs, they were excluded.

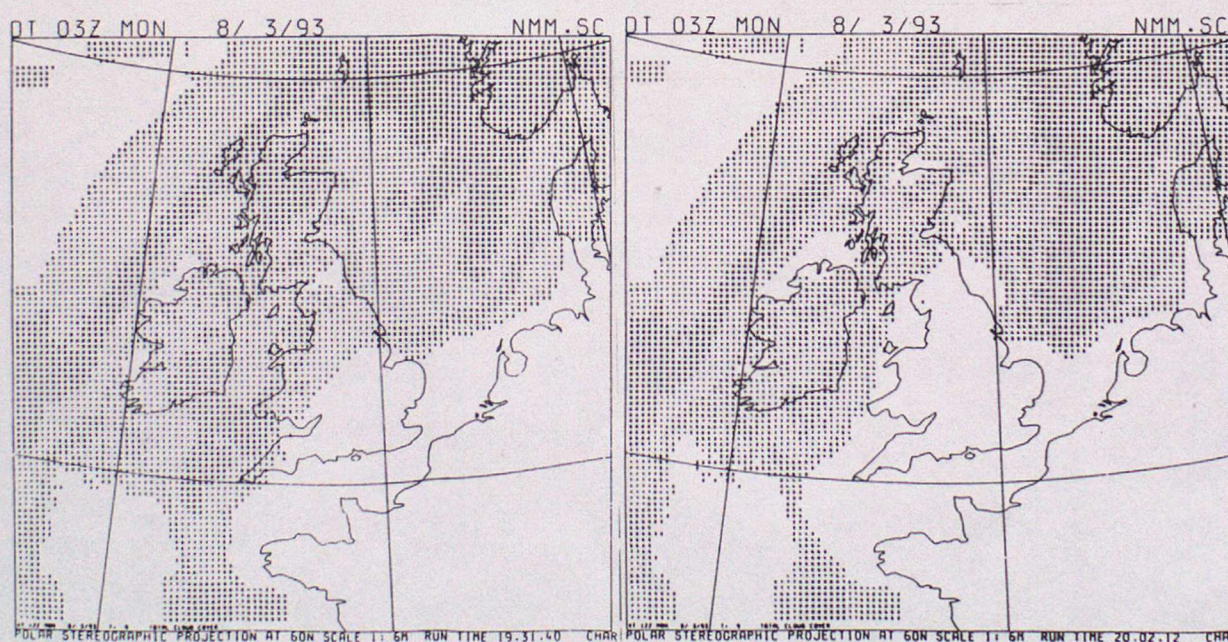
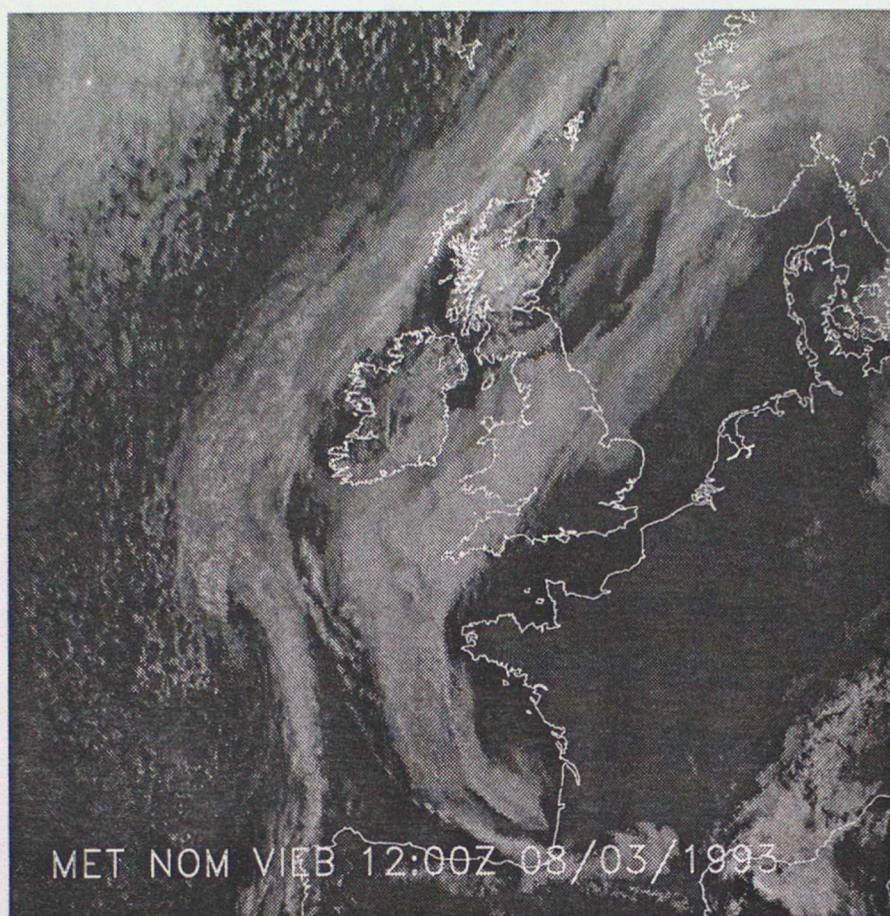
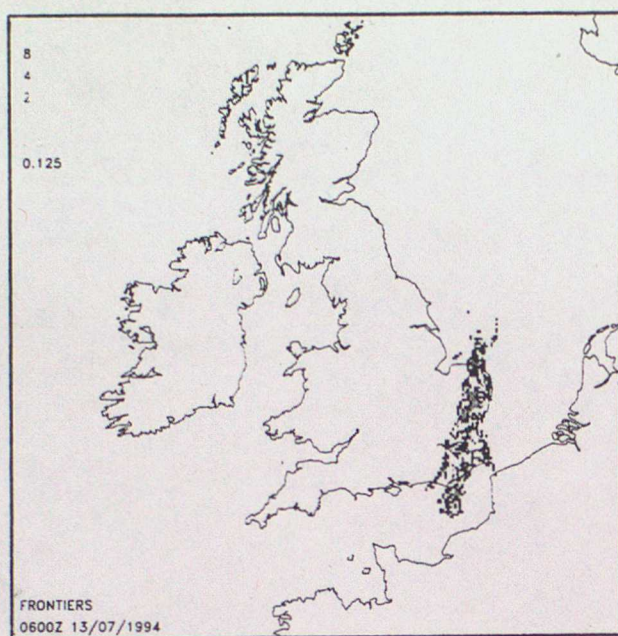
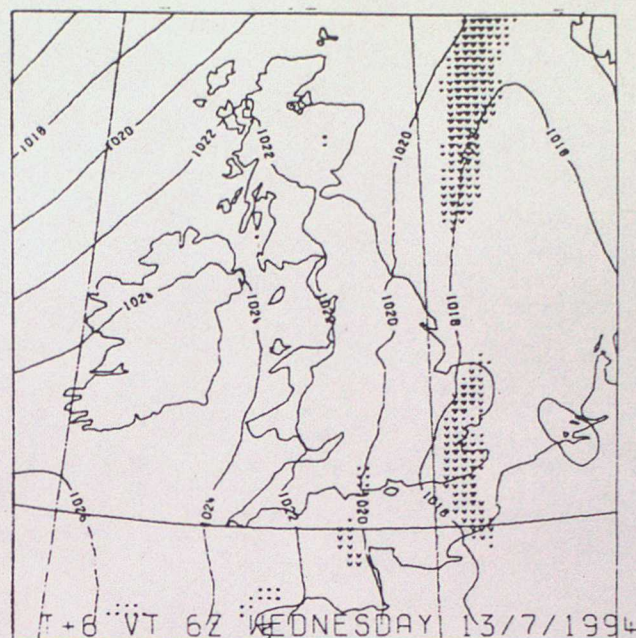


Figure 13: An impact on forecast total cloud cover from assimilating MOPS cloud data. The top panel shows the Meteosat visible image for 12 UTC on 8th March 1993, when a stratocumulus sheet covered northern and central England, Wales and the south-west approaches, with frontal cloud to the north-west. The bottom two frames show 6-hour mesoscale model forecasts from 6 UTC data times, with areas of total cloud cover ≥ 3 oktas shaded: left: from analysis *including* MOPS data
right: from analysis *excluding* MOPS data
Radiosonde humidity data were omitted from both runs.



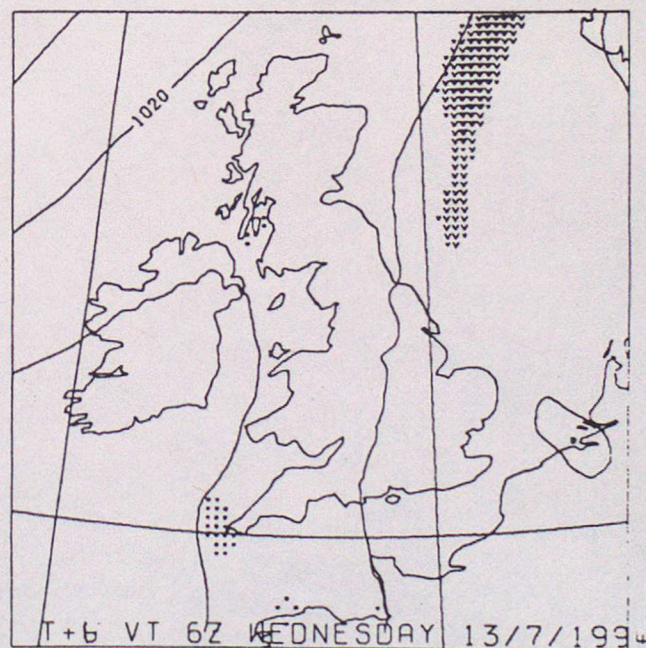
(a)



(b)

Figure 14: Beneficial impact from the assimilation of MOPS cloud data on a precipitation forecast.

- (a) composite radar image for 6 UTC 13th July 1994.
- (b) 6-hour mesoscale model forecast from data time 0 UTC.
- (c) as (b) *without* assimilation of MOPS data.



(c)

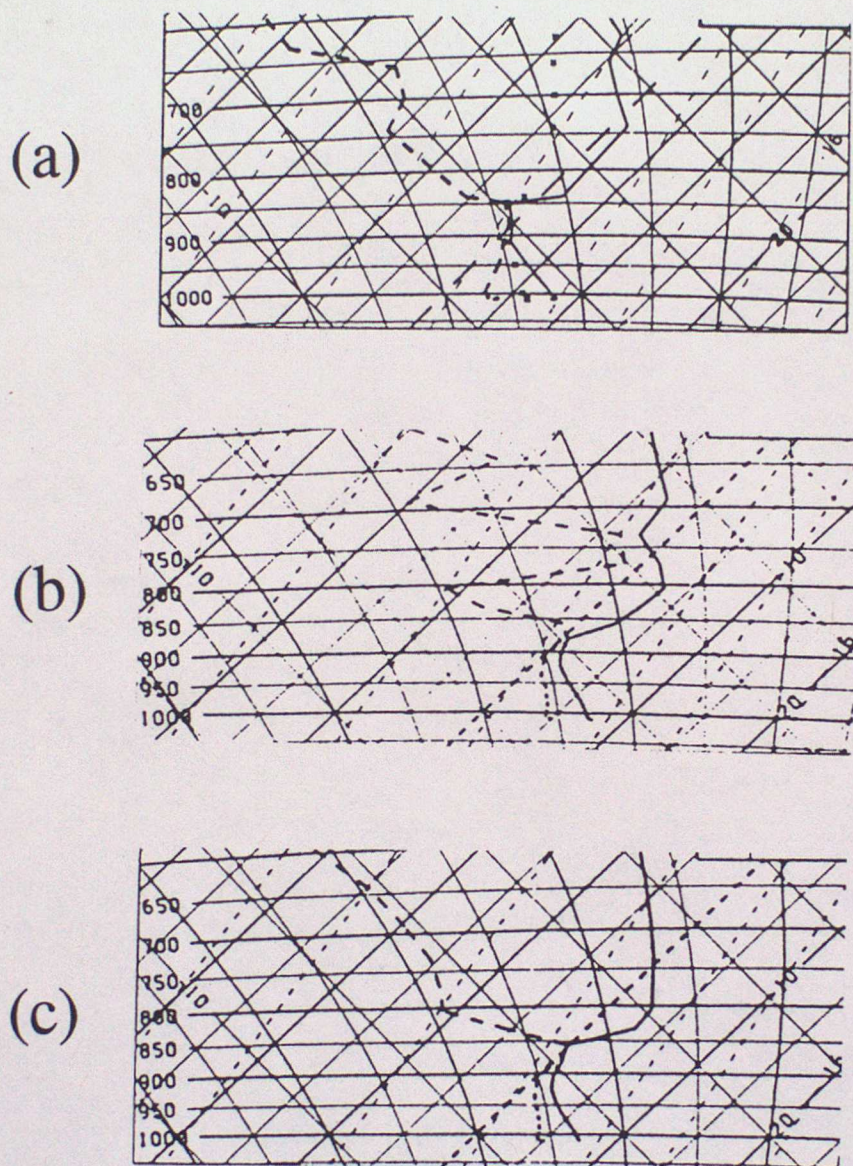


Figure 15: Impact of different cloud top height assignment techniques within MOPS on forecast moisture profiles for a stratocumulus situation.

- (a) observed sounding for Camborne at 12 UTC 7th March 1993.
- (b) 6-hour mesoscale model forecast from data time 6 UTC, with cloud top height in MOPS assigned by searching the model background temperature profile for a temperature matching the satellite brightness temperature.
- (c) as (b) with height assignment via the conceptual model described in Section 6(a).

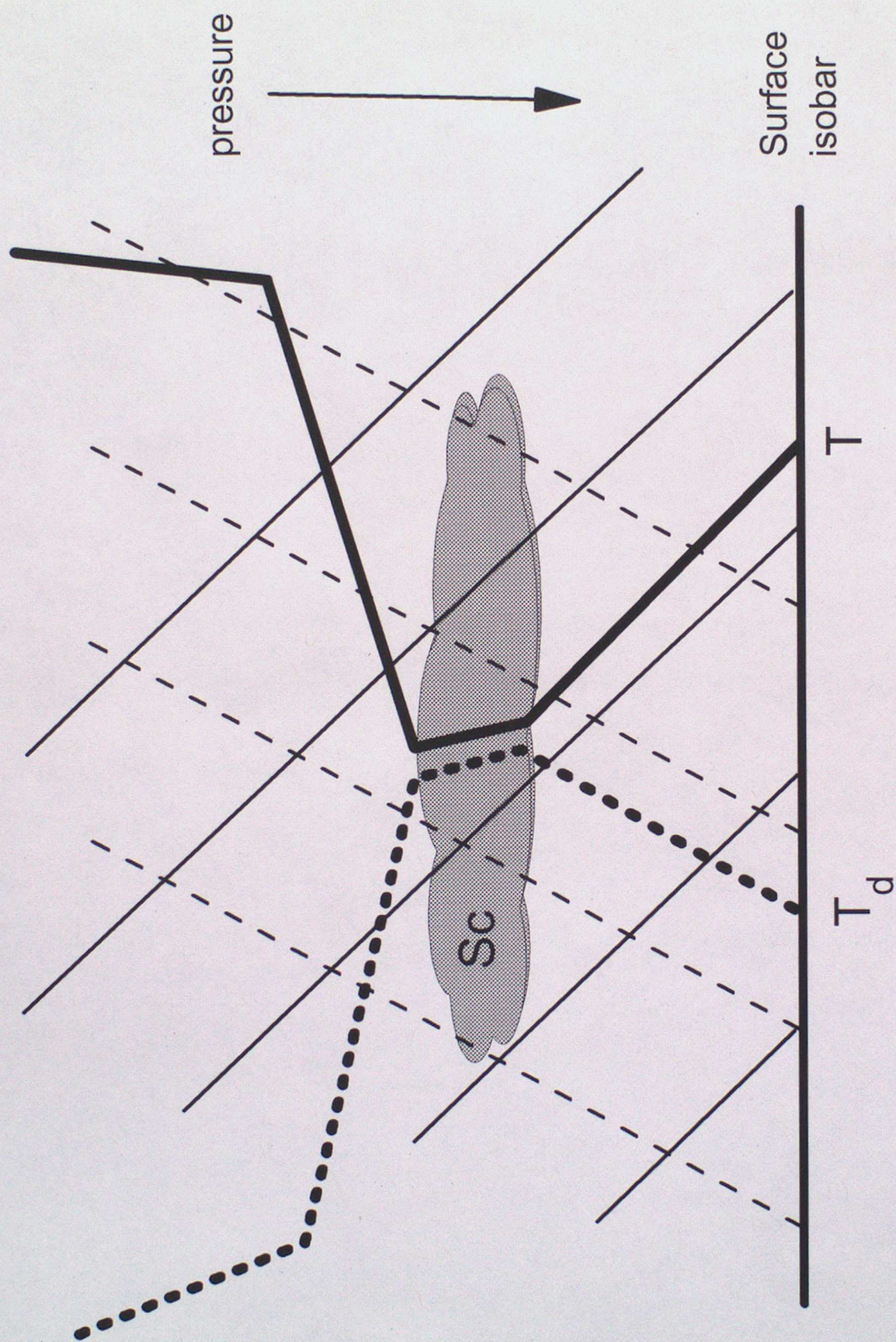


Figure 16: Idealised tephigram through a layer of stratocumulus (Sc) cloud.

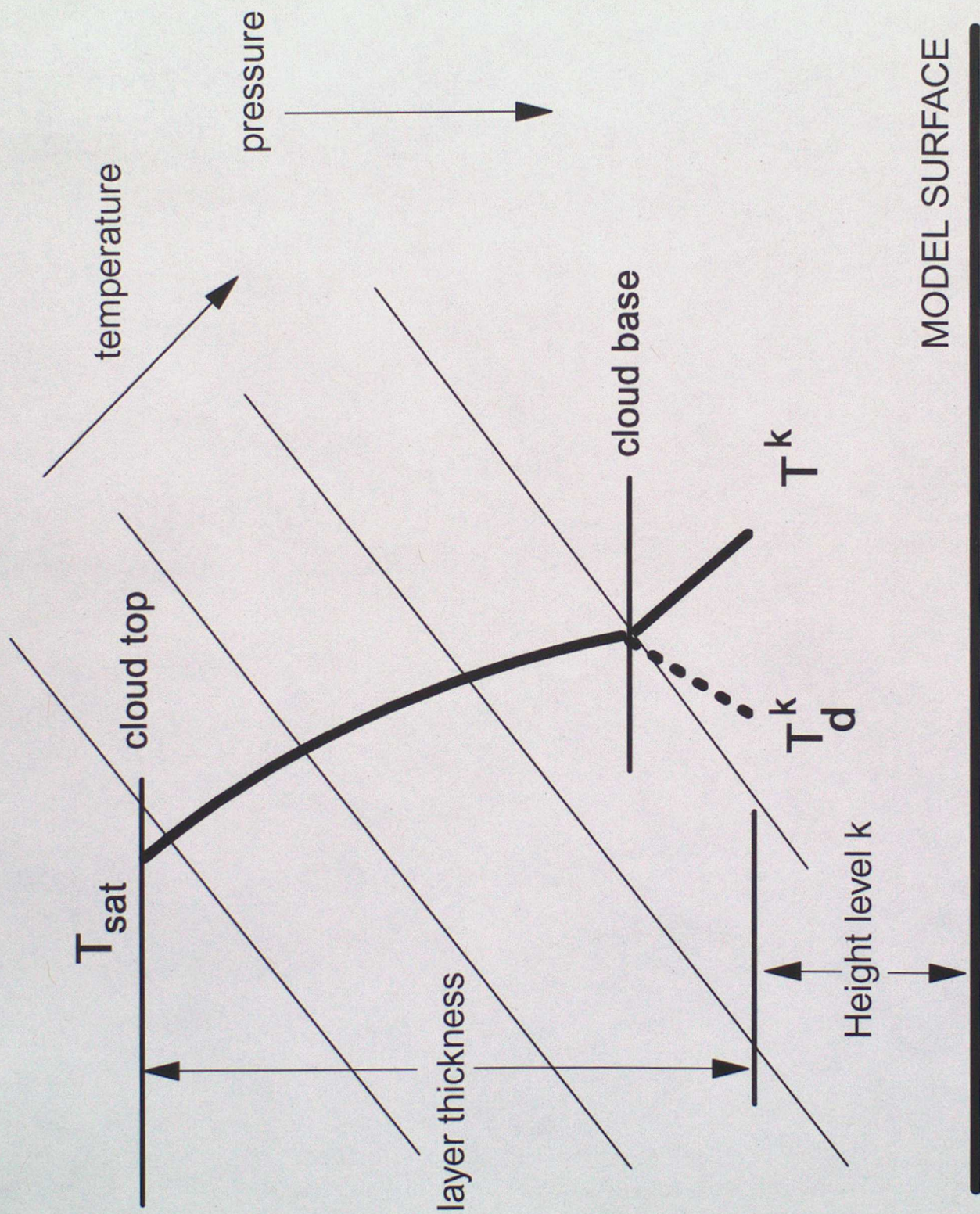
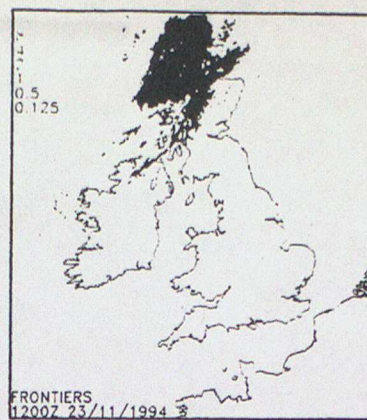
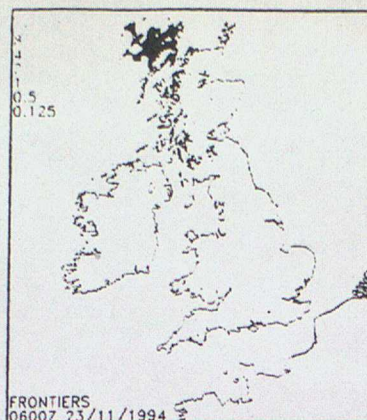
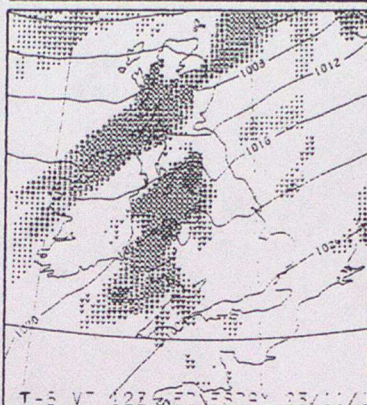
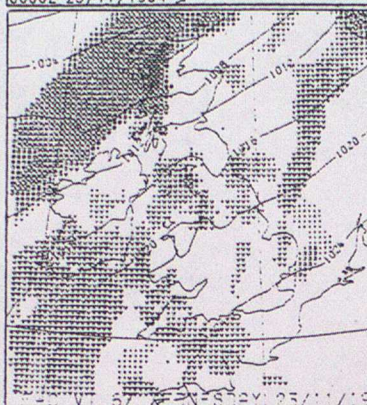


Figure 17: Application of the idealised profiles in Figure 16 to the derivation of cloud top height for low cloud in the MOPS analysis.

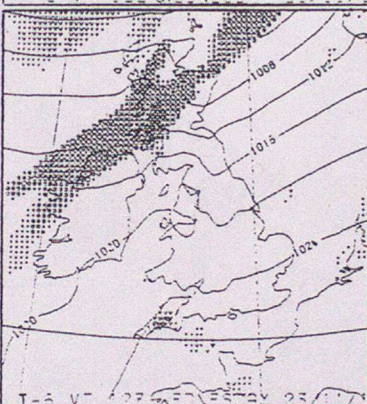
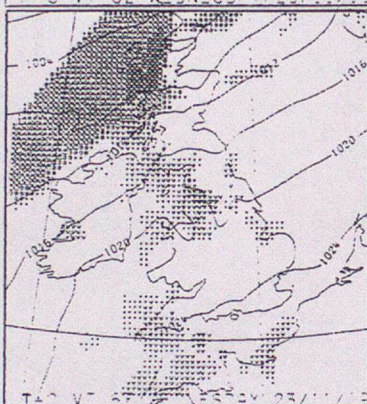
(a)



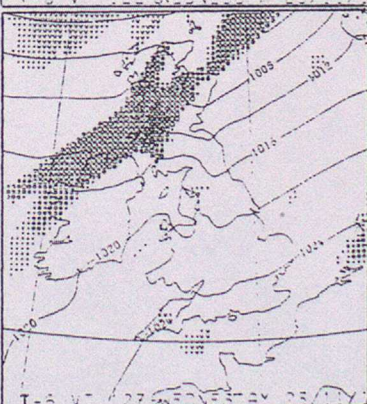
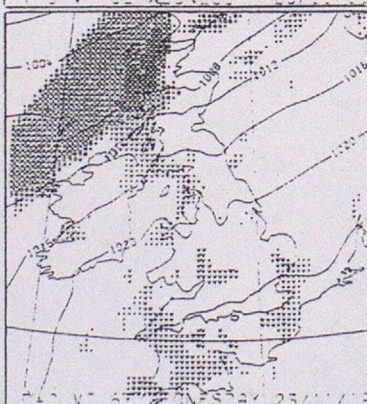
(b)



(c)



(d)



T+0

T+6

Figure 18: Effect of different treatments of Meteosat imagery within MOPS on a precipitation forecast.

- (a) composite radar imagery for 23rd November 1994 at 6 UTC (left) and 12 UTC (right)
- (b) analysis and 6-hour (CONTROL) forecast from data time 6 UTC
- (c) as (b) but *without* use of Meteosat imagery in MOPS (noSAT run)
- (d) as (b) but model background high cloud used for quality control within MOPS, to determine areas where Meteosat imagery may change cloud amounts but *not* cloud heights (qcSAT run)

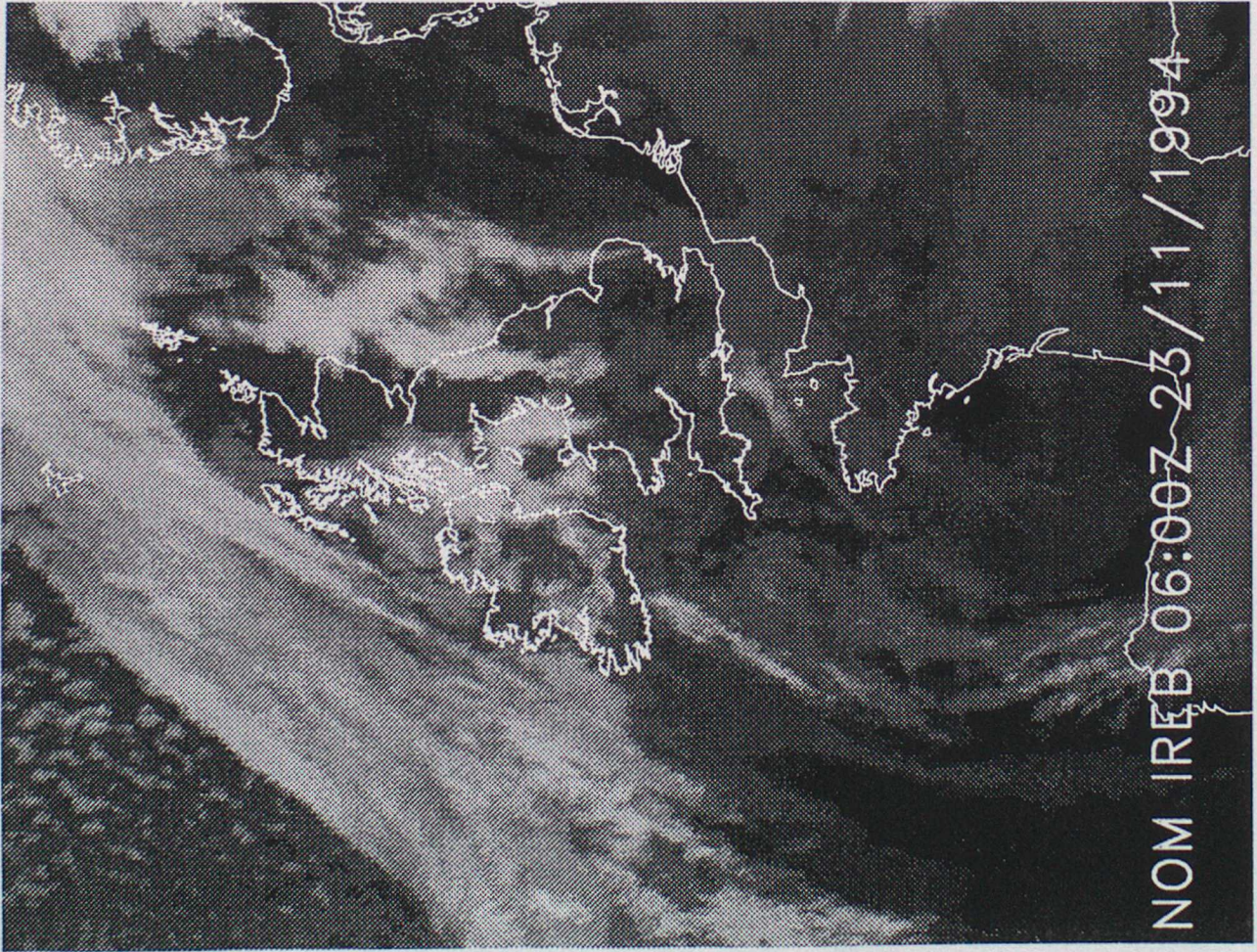


Figure 19

3-hour mesoscale model forecast of
'high' cloud from data time 3 UTC.
Black areas have no high cloud, brightest
areas have most high cloud.

Meteosat infrared image for 6 UTC 23rd
November 1994